

Late Miocene–Quaternary fault evolution and interaction in the southern California Inner Continental Borderland

Christopher C. Sorlien¹, Jonathan T. Bennett^{2,*}, Marie-Helene Cormier^{2,†}, Brian A. Campbell², Craig Nicholson³, and Robert L. Bauer²

¹Earth Research Institute, 6832 Ellison Hall, University of California–Santa Barbara, Santa Barbara, California 93106, USA

²Department of Geological Sciences, 101 Geological Sciences Building, University of Missouri, Columbia, Missouri 65211, USA

³Marine Science Institute, University of California–Santa Barbara, Santa Barbara, California 93106, USA

ABSTRACT

Changing conditions along plate boundaries are thought to result in the reactivation of preexisting structures. The offshore southern California Borderland has undergone dramatic adjustments as conditions changed from subduction tectonics to transform tectonics, including major Miocene oblique extension, followed by transpressional fault reactivation. However, consensus is still lacking about stratigraphic age models, fault geometry, and slip history for the near-offshore area between southern Los Angeles and San Diego (California, USA). We interpret an extensive data set of seismic reflection, bathymetric, and stratigraphic data from that area to determine the three-dimensional geometry and kinematic evolution of the faults and folds and document how preexisting structures have changed their activity and type of slip through time. The resulting structural representation reveals a moderately landward-dipping San Mateo–Carlsbad fault that converges downward with the steeper, right-lateral Newport–Inglewood fault, forming a fault wedge affected by Quaternary contractional folding. This fault wedge deformed in transtension during late Miocene through Pliocene time. Subsequently, the San Mateo–Carlsbad fault underwent 0.6–1.0 km displacement, spatially varying between reverse right lateral and transtensional right lateral. In contrast, shallow parts of the previously identified gently dipping Oceanside detachment and the faults above it appear to have been inactive since the early Pliocene. These observations, together with new and revised geometric representations of additional steeper faults, and the evidence for a pervasive strike-slip component on these nearshore faults, suggest a need to revise the earthquake hazard estimates for the coastal region.

INTRODUCTION

Prominent continental transform fault systems, such as the San Andreas (California, USA; e.g., Crowell, 1979), the North Anatolian in northwest Turkey (e.g., Şengör et al., 2005), and the Marlborough in New Zealand (e.g., Roberts, 1995) are characterized by broad zones of distributed faulting. These faults

*Present address: Apache Corporation, 6120 S. Yale Avenue, #1500, Tulsa, Oklahoma 74136, USA

†Present address: Graduate School of Oceanography, University of Rhode Island, 215 S. Ferry Road, Narragansett, Rhode Island 02882, USA

commonly reactivate preexisting structure (Görür and Elbek, 2014; Crowell, 1950), and thus may be unfavorably oriented for the current stress and strain. For example, moderately dipping strike-slip faults with displacements from a few kilometers to >100 km are well documented in California. These faults include the large-displacement San Gregorio fault found off the city of Santa Cruz (Langenheim et al., 2012), the southern San Andreas fault (Nicholson, 1996; Fuis et al., 2012), and the Santa Monica–Dume fault offshore Malibu (Sorlien et al., 2006). New steeper parts of strike-slip faults may form locally or regionally, and dip-slip components may partition onto the older flatter fault sections (Mount and Suppe, 1992; Lettis and Hanson, 1991). Strike-slip components of slip can be revealed by patterns of uplift or subsidence, and shortening and extension, linked to map-view fault bends (e.g., Crowell, 1974). Such deformation is focused on hanging walls of nonvertical faults, especially moderately dipping ones (Seeber et al., 2006; Kurt et al., 2013).

Patterns of shortening and extension along transform systems are dramatically illustrated in the offshore domain of southern California. During the past 20 m.y., this part of the diffuse plate boundary has evolved from accommodating microplate subduction to a complex dextral transform boundary. A 200-km-long crustal block underwent $\geq 90^\circ$ of clockwise vertical axis block rotation, accompanied by major oblique extension and then by oblique shortening (Kamerling and Luyendyk, 1985; Crouch and Suppe, 1993; Nicholson et al., 1994). This complex history, especially post-Miocene oblique convergence, resulted in a broad zone of deep basins, submerged ridges, and islands called the California Continental Borderland. The Inner Borderland corresponds to the ~100-km-wide zone closest to shore (Fig. 1A). It is composed of erosionally and tectonically denuded Catalina Schist overlain by Miocene and younger sedimentary and volcanic rocks (Fig. 2; e.g., Vedder, 1987). Miocene extension was accommodated on gently north-north-east– to east-northeast–dipping faults, which have been documented within 50 km of the present coast between Santa Monica and San Diego (Nicholson et al., 1993; Crouch and Suppe, 1993; Bohannon and Geist, 1998; Rivero et al., 2000; Sorlien et al., 2013). Post-Miocene oblique convergence progressively overprinted and reactivated these earlier fault structures, causing basin inversion and fold development in the northern part of the Inner Borderland and Los Angeles basin (Wright, 1991; Yeats and Beall, 1991; Schneider et al., 1996; Seeber and Sorlien, 2000; Rivero and Shaw, 2011). The net result of this evolving plate boundary geometry and plate boundary conditions is that

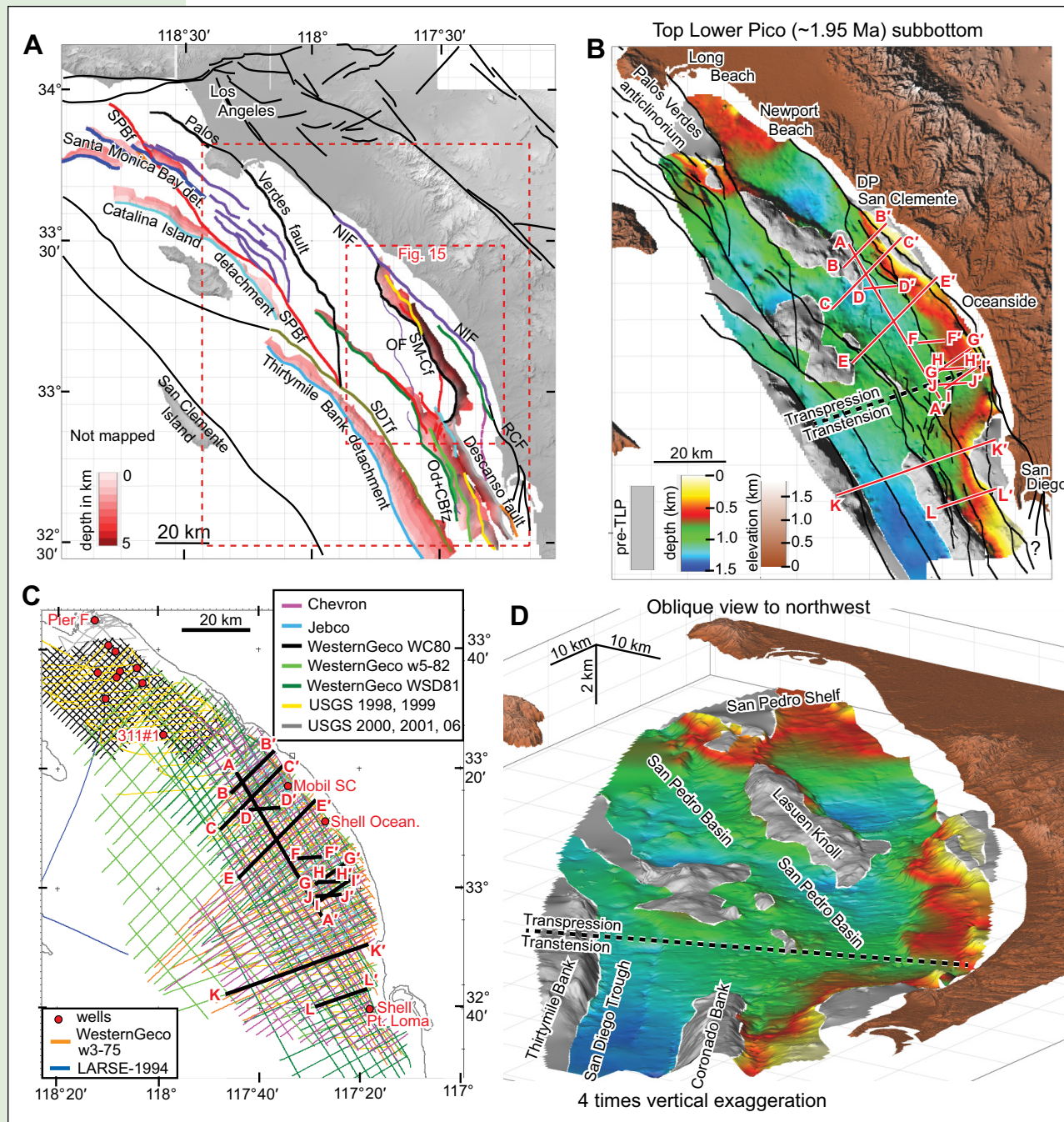


Figure 1. (A) A regional map of Quaternary faults. Faults are from Sorlien et al. (2010, 2013), Wright (1991), Plesch et al. (2007), and this study. The thin purple lines indicate mapped locations of the Oceanside fault (OF) of Rivero et al. (2000), from Plesch et al. (2007, as modified by Sorlien et al., 2010). The Inner California Continental Borderland is the offshore area shown east of San Clemente Island and adjacent San Clemente fault. Od+CBfz—Oceanside detachment and Coronado Bank fault zone; NIF—Newport-Inglewood fault; RCF—Rose Canyon fault; SDTF—San Diego Trough fault; SM-Cf—San Mateo-Carlsbad fault; SPBF—San Pedro Basin fault; det.—detachment. Outer dashed red rectangle locates B, C, and D; inner labeled dashed red rectangle locates Figure 15. (B) Top lower Pico (TLP; ca. 1.95 Ma) subbottom horizon is in color. Gray is where TLP has overlapped older strata in the subbottom and/or where older strata crop out at the seafloor. Seismic reflection profiles A–A' through L–L' are in red. The labeled east-northeast–west-southwest heavy black dashed line is the boundary between late Quaternary transpression (north) and transtension (south). DP—Dana Point. (C) The data set of multichannel seismic reflection profiles, identified in the legend. Locations of figures are heavy black lines. Wells (red circles) are from Sorlien et al. (2013) and this study. LARSE—Los Angeles Regional Seismic Experiment (<http://woodshole.er.usgs.gov/operations/obs/larse94.html>); Mobil SC—Mobil San Clemente 1; Shell Ocean.—Shell Oceanside 1; USGS—U.S. Geological Survey. (D) Oblique view to northwest of most of the same TLP depth model shown in B.

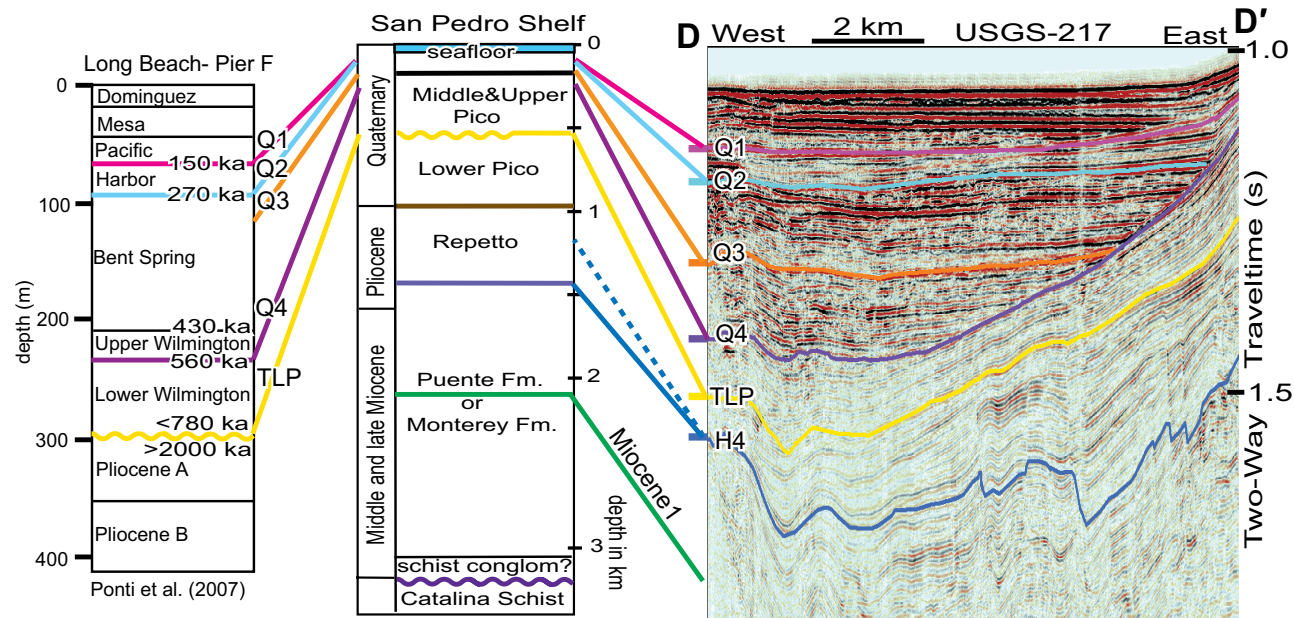


Figure 2. U.S. Geological Survey (USGS) high-resolution multichannel seismic reflection profile showing the interpreted horizons (in Fig. 1 as D–D' in the footwall southwest of the San Mateo–Carlsbad fault). Quaternary 4 (Q4) here is a major onlap surface representing increasing missing section to the east. The stratigraphic column in the center is modified from Wright (1991) for the downthrown northeast side of the Palos Verdes fault on the San Pedro shelf, south of Long Beach. The Quaternary horizons were correlated as part of this project to a scientific corehole on Pier F of the port of Long Beach (Ponti et al., 2007; Edwards et al., 2009) (far left). Late Quaternary ages (post-780 ka) are from Ponti et al. (2007). Fm.—formation; conglom—conglomerate.

multiple generations of fault sets have developed that mutually interact and, in some cases, segment each other and influence how older fault sets are or have been reactivated.

How three-dimensional (3D) fault geometry affects kinematics, including fault abandonment and reactivation, is also important. In this study, fault geometry and slip history are investigated for an offshore system of stacked downward-converging linked faults that extends from Newport Beach to San Diego, within 20–30 km of the modern coast (Fig. 1). Earthquake hazard to cities and facilities along the coast is related to which parts of which faults exhibit ongoing activity, and what slip types and slip rates characterize these segments. There has been little published agreement on fault slip type, continuity, existence, and age of deformed sedimentary rocks in this area. One controversial fault has been called the Oceanside thrust (Rivero et al., 2000; Rivero and Shaw, 2011), part of which coincides with the Oceanside detachment of Bohannon and Geist (1998; presented but not named in Crouch and Suppe, 1993). Its 110 km length and 1800 km² area north of the offshore Mexican border suggests a potential for major earthquakes and tsunami hazard should this entire fault surface be currently active and rupture in a single

event (Rivero et al., 2000; Plesch et al., 2007; Rivero and Shaw, 2011). Alternatively, its north-striking central segment has been interpreted as abandoned, and Miocene extension is not overprinted (Sorlien et al., 2010; Bennett, 2012; see Ryan et al., 2009).

The Oceanside detachment is at a higher structural level above another major Miocene detachment fault, the Thirtymile Bank detachment (e.g., Bohannon and Geist, 1998). Including its misaligned or offset northwestern continuation, the Catalina Island detachment (Sorlien et al., 2013), the lower detachment level is at least 180 km long in United States waters (Fig. 1A), and continues farther in Mexican waters (Legg, 1985). It has also been proposed that this fault has been reactivated as the Thirtymile thrust (Rivero et al., 2000).

There are few estimates for Quaternary fault slip rates of Inner Borderland faults. Such estimates can depend on knowing the age of deformed sedimentary rocks. Sedimentary age models for the 500 m below the seafloor are both old (Crouch and Suppe, 1993; Sorlien et al., 2010; Rivero and Shaw, 2011) and young (Covault and Romans, 2009; Normark et al., 2009) interpretations. These age model differences of between a few times to an order of magnitude would

result in similar differences in fault slip rate estimates implied by deformed and offset sedimentary rocks.

DATA SOURCES

The primary data set used in this study was grids of industry multichannel seismic reflection (MCS) profiles acquired by Western Geophysical, Chevron, and Jebco during the late 1970s through 1980s. These data were made publicly available in recent years through the National Archive of Marine Seismic Surveys (<http://walrus.wr.usgs.gov/NAMSS>; Hart and Childs, 2005). Higher resolution MCS profiles collected by the U.S. Geological Survey (USGS) in 1998, 1999, 2000, 2001, and 2006 were also utilized (Sliter et al., 2005, 2010; Fig. 1C). A bathymetric grid was compiled from point and multibeam bathymetric data (Dartnell and Gardner, 1999; National Geophysical Data Center: <http://www.ngdc.noaa.gov/mgg/bathymetry/>). This grid was used as the basis for identifying recent seafloor deformation, and for registering and correcting the location

of seismic reflection profiles where the relation between stacked trace number and shotpoint navigation proved problematic.

Age control needed to assess the history of fault and fold activity was provided by correlation to data collected from deep-penetrating hydrocarbon wells. Well data include velocity surveys for depth-to-time conversion, paleontology from the U.S. Minerals Management Service (now U.S. Department of the Interior Bureau of Ocean Energy Management and Bureau of Safety and Environmental Enforcement, BOEM and BSEE), and formation tops from industry well reports or lithologic description (i.e., mud logs) (for data sources and references, see the supplementary appendix in Sorlien et al., 2013; publicly available well log database from the BOEM or BSEE). Deep scientific coreholes in and near Los Angeles and Long Beach Harbors provided additional detailed dated stratigraphy, especially since the last magnetic reversal ca. 780 ka (Fig. 2; Ponti et al., 2007; Edwards et al., 2009; Ehman and Edwards, 2014; McDougall et al., 2012). This direct seismic stratigraphic correlation results in significantly older age estimates for sedimentary units than previous interpretations based on a seismic stratigraphic model (Fig. 3).

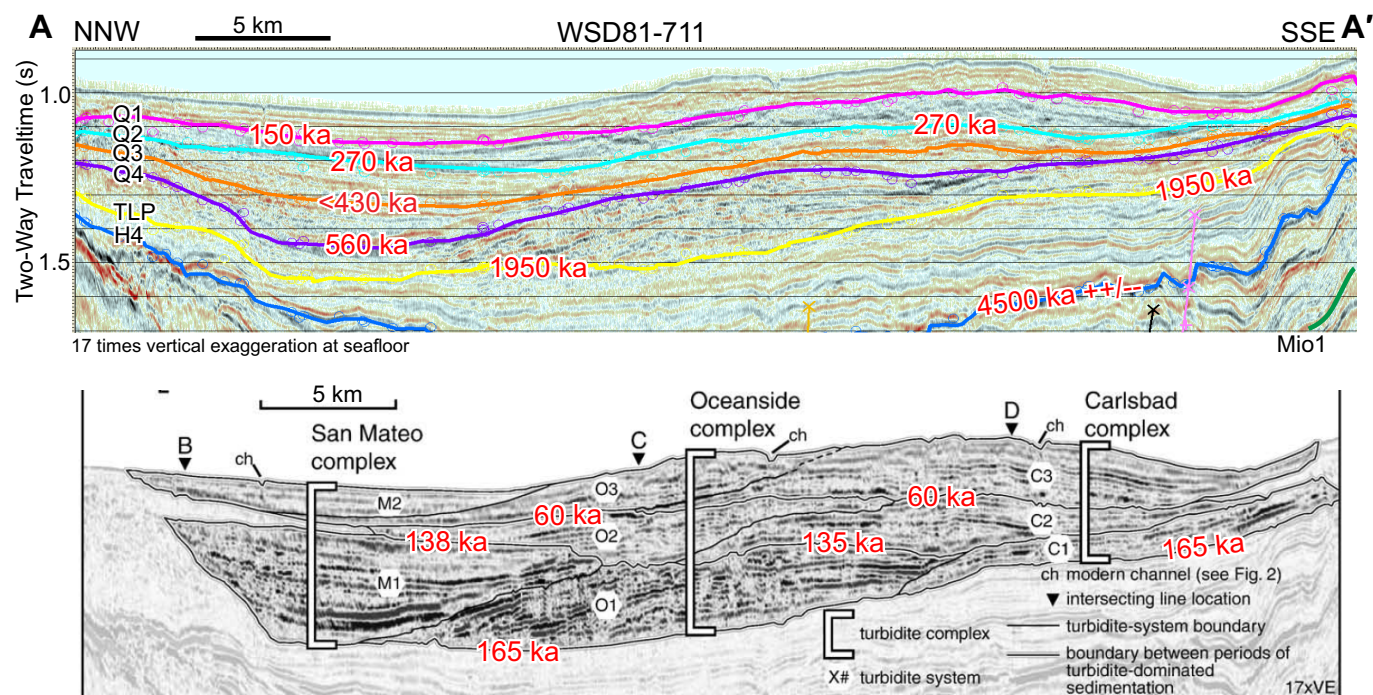


Figure 3. Profile A–A', located in Figure 1, comparing two age models for the offshore Inner Borderland. Our interpretation is at the top and the Covault and Romans (2009) interpretation is at the bottom, with addition of ages using Covault and Romans (2009, Fig. 5 therein). VE—vertical exaggeration.

METHODS

Structural and Stratigraphic Interpretation

Seismic-stratigraphic and fault interpretation was carried out using interactive industry software, IHS Kingdom Suite (<https://www.ih.com>). Loop tying of seismic stratigraphy and faults was done at all intersections of all 2D MCS profiles. Owing to the close line spacing (1–2 km) of the combined grids of MCS profiles, detailed 3D representations of stratigraphic horizons and fault surfaces were produced with high confidence.

Within a zone of nonvertical faults, we generally mapped the deepest (underlying) fault that deformed Quaternary strata, and did not interpret smaller, but potentially active strands, at shallower levels even if they deformed the seafloor. Many of the shallow faults project downward to intersect and merge with the faults we mapped and represented as 3D depth-converted grids.

Gridding, Depth Conversion, and Cross Sections

Five distinct Quaternary seismic-stratigraphic reference horizons, Q1–Q4 and the top lower Pico (TLP) were interpreted (Fig. 2). Interpretations of stratigraphic horizons and faults were gridded and then depth converted. The Harvard version of the Southern California Earthquake Center Community Velocity Model (CVM-H; <http://structure.rc.fas.harvard.edu/projects/cvm-h/>) was used for the depth conversion (Süss and Shaw, 2003; Bennett, 2012). Cross sections ($n = 58$) spaced at 1 km were produced through the depth model of faults and stratigraphy. These cross sections are perpendicular to the overall strike of the San Mateo–Carlsbad fault. Farther south, including offshore San Diego, additional cross sections spaced at 5 km were constructed to illustrate the changing geometry along strike of the strands of the Coronado Bank–Descanso fault system.

Estimating Fault Displacement

Although measuring or modeling shortening from faulting and folding can be fairly straightforward using 2D MCS profiles, accurately estimating fault displacement, including possible strike-slip components, is more problematic. To better estimate fault displacement, we take advantage of the fact that a nonvertical strike-slip fault with bends along strike will exhibit varying components of dip slip along strike. Based on our experience, moderately dipping faults like the San Mateo–Carlsbad fault are most suitable for kinematic analysis because most deformation including structural relief growth is limited to the fault and its hanging wall (e.g., Sorlien et al., 2006). If the 3D geometry of a suitable fault is known, and the structural relief due to faulting and local folding of a dated horizon is also known, then it is a relatively simple trigonometric problem to figure out the fault displacement, including its

slip direction. Along nonvertical transtensional or transpressional faults, the vertical structural relief, SR, resulting from oblique slip on the fault plane can be derived from:

$$SR = (\text{horizontal slip distance}) * \sin \alpha * \tan \delta, \quad (1)$$

where α is the angle between the horizontal component of slip and the fault strike, and δ is the true dip of the fault plane (Fig. 4). For the more realistic case where both fault strike and fault dip vary spatially rather than remain constant, such as along the Carlsbad fault system, the resulting vertical deformation can be derived by adding each bit of relief that develops locally as slip proceeds through a succession of n fault segments:

$$SR = \sum_{i=1}^n L_i * \sin \alpha_i * \tan \delta_i, \quad (2)$$

where the subscript i refers to the i -th fault segment, L_i indicates the length of that segment, and n indicates the number of fault segments through which slip has proceeded.

Where the 3D geometry of a fault is known, the expected structural relief that would develop along that fault can be derived for a range of total displacements or displacement directions. In turn, by comparing modeled and observed structural relief along dated stratigraphic horizons, the slip parameters that best reproduce the observations can be adequately estimated, an approach that was successfully applied to the Santa Monica–Dume fault system (Sorlien et al., 2006).

We apply that same trigonometric approach to quantify the horizontal component of displacement and displacement azimuths along the San Mateo–Carlsbad fault for the past ~2 m.y. We measured the structural relief of the top lower Pico sequence boundary, the strike of the 2.5 km depth contour of the fault surface, and dip of the fault at each of the 58 cross sections. A depth of 2.5 km was chosen for the strike measurement because it avoids the shallow irregularities in the fault, and it is also approximately centered beneath the part of the hanging wall where structural relief was measured. The relief due to faulting and folding was measured within 2 km of the fault tip in its footwall and within 4 km in its hanging wall. Strikes, dips, and relief were further interpolated between cross sections every 200 m, so that the struc-

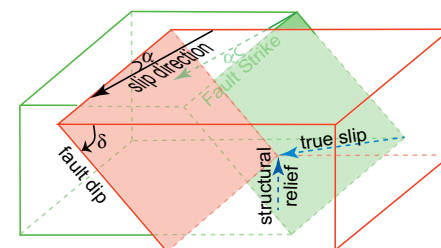


Figure 4. A block representation of the parameters used for calculating structural relief. This example illustrates oblique reverse right-lateral slip. The slip direction is measured in a horizontal plane.

tural relief accumulated for a range of given displacements along a particular displacement direction could be calculated from an extension of Equation 2 as follows:

$$SR = \sum_{i=1}^n (200 \text{ m}) * \sin \alpha_i * \tan \delta_i, \quad (3)$$

where SR is the cumulative vertical relief that develops from slip across n adjacent 200-m-wide corridors, and the index i refers to an individual 200-m-wide corridor. The parameter n is adjustable to simulate varying amount of horizontal displacement on the fault. The modeled structural reliefs for a range of horizontal displacements and displacement directions are then graphed against the measured structural relief, and best matches are visually chosen. (For further details about this method, see Bennett, 2012.)

Because earthquake hazard is more directly related to the true fault displacements in the plane of the fault rather than to its horizontal component, we assess that true displacement from the horizontal component of displacement as:

$$\text{True Displacement} = (\text{horizontal displacement}) * \sqrt{1 + (\sin^2 \alpha * \tan^2 \delta)}. \quad (4)$$

To assess whether late Quaternary fault slip rate and direction have been similar to the post ca. 1.95 Ma average, the structural relief of the Q3 and Q4 horizons across the fault system was also measured. It was only possible to completely interpret these horizons in the hanging wall of the San Mateo–Carlsbad fault for ~25 km along its strike. Because folding of Q3 and Q4 does not extend very far from the fault along that 25 km, their relief was measured within 2 km of the fault tip for the hanging wall and 1 km for the footwall.

Sources of Error

Error in the two-way traveltime fault and stratigraphic interpretations was minimized during this study by systematically closing the thousands of ties at the intersections between all the MCS profiles. However, unconformities can be time transgressive and therefore may be of slightly different age in the basin than where they are dated at wells or cores. With only three wells over much of the study area, the CVM-H velocity model is presumably mainly based upon stacking velocities derived from processing of MCS data, rather than true interval P-wave velocities from refraction studies or velocity surveys in wells (Süss and Shaw, 2003; <http://structure.rc.fas.harvard.edu/projects/cvm-h/>). The velocity model therefore may contain significant error, perhaps as high as 10% (e.g., Hughes, 1985). The trigonometry used in the slip modeling assumes that the hanging wall is moving rigidly (obliquely) up or down the apparent dip of the footwall. However, for fault-propagation folds, shallow structural relief can be greater than the vertical component of fault slip at depth (Hubbard et al., 2014). This can result in our trigonometric modeling overestimating displacement by up to a factor of two where a broad forelimb develops above a blind fault.

RESULTS

Stratigraphic Interpretation

In the absence of any publicly available well data that directly sample Quaternary sedimentary rocks south of the San Pedro shelf and offshore Newport Beach (Fig. 1), stratigraphic age models remain subject to debate. The one exception is the Shell Point Loma well near San Diego, but the available information lacks good age control for the Quaternary. Normark et al. (2009) and Covault and Romans (2009) proposed an age model that relies on the correlation of depositional cycles to the global sea-level record below shallow radiocarbon dated cores (Fig. 3). Our approach involves seismic stratigraphic correlations to data from both distant and nearby industry wells and scientific coreholes (Fig. 1C). This approach has allowed us to identify, map, and date five distinct Quaternary seismic-stratigraphic reference horizons, Q1–Q4 and the top lower Pico (TLP; Fig. 2). We selected our four Q sequence boundaries on the high-resolution USGS MCS data in the area of D–D' (Fig. 2), and later correlated them regionally, including a correlation to the Pier F corehole (Bennett, 2012). We also compared our correlation of these horizons across the San Pedro shelf to the seismic stratigraphic interpretation of Ehman and Edwards (2014), and the two age models agree. An early Pliocene horizon (H4) and a Miocene horizon (Miocene1) were also identified in two wells offshore Oceanside and San Clemente, respectively (Fig. 1). A composite seismic reflection profile showing the continuous correlation of stratigraphy from Long Beach Harbor Pier F corehole, south-southeast for a distance of 130 km, is available in Bennett (2012; Fig. 1C). All six interpreted horizons are available as text files in the Supplemental File¹, and an included “Read Me” file explains the format.

Our 1950 ± 15 ka age for the top lower Pico horizon (Blake, 1991; Sorlien et al., 2013) is more than an order of magnitude older than the age of strata immediately above it, as interpreted by Covault and Romans (2009) (Fig. 3). Our Q1–Q4 sequence boundaries are also several times older. This revised age model is consistent with interpretations of Crouch and Suppe (1993) and Rivero and Shaw (2011) that, like us, used seismic stratigraphic correlations correlated directly to petroleum well data. Our age model comes from careful seismic reflection profile-to-well correlations using all resolutions of seismic profiles within the broader study area. In contrast, the young age model of Covault and Romans (2009) is not based on direct dating below the ~40 k.y. range of radiocarbon dating (Normark et al., 2009).

The younger age model of Covault and Romans (2009) may result from missing and merged sequence boundaries from the succession of glacial-interglacial cycles in the stratigraphic record. One such example is the onlap of hundreds of meters of sediment onto Q4 in Figure 2, producing a hiatus much longer than a 100 k.y. glacial cycle. Another example is a scientific corehole at Pier F in Long Beach Harbor that sampled post–780 ka strata above an unconformity and pre–2 Ma strata below it (Fig. 2; Ponti et al., 2007; Edwards et al., 2009). This unconformity splits southward into several additional boundaries,

Sorlien, C.C., Bennett, J.T., Cormier, M.H., Campbell, B.A., Nicholson, C., and Bauer, R.L., 2015. Late-Miocene–Quaternary fault evolution and interaction in the southern California Inner Continental Borderland. *Geosphere*, v. 11, doi:10.1130/GES01118.1.

Supplemental text files for: Late-Miocene–Quaternary fault evolution and interaction in the Southern California Inner Continental Borderland. <http://dx.doi.org/10.1130/GES01118.1>

Christopher C. Sorlien, Jonathan T. Bennett, Marie-Hélène Cormier, Brian A. Campbell, Craig Nicholson, Robert L. Bauer

The stratigraphic interpretation is provided as seven text files, one for each horizon. Rather than export a point for every seismic trace, a point approximately every 100 m along each profile is provided. We have found that having very close point spacing along a profile and large distances between profiles produces artifacts in gridding. Additionally, the 100 m spacing results in much smaller file sizes. The horizons were originally exported from IHS-Kingdom Suite. Version 8.8 and earlier versions of this software export shot number rather than sequential trace number. Therefore, the files consist of Line name, shot number, X, Y, and two-way time in seconds. The X and the Y are UTM Zone 11 NAD83. Files in this format can be imported back into IHS Kingdom Suite, OpenText, and similar software. However, the line names must match. Alternatively, the X, Y Time points can be gridded and the grids imported.

Because of the large scope of this work, the seismic stratigraphic interpretation is not “polished”. That means that there are many small “mistakes” (vertical shifts) at line intersections.

¹Supplemental File. Zipped text files of the stratigraphic horizon interpretations along seismic reflection profiles and as grids in time and in depth, and fault interpretations. Please visit <http://dx.doi.org/10.1130/GES01118.S1> or the full-text article on www.gsapubs.org to view the Supplemental File.

including our top lower Pico and one or more unconformities that we did not interpret. Our ca. 2 Ma age for our top lower Pico horizon results in estimates of deformation rates that are also an order of magnitude slower than would be implied by the age model of Covault and Romans (2009).

Our H4 sequence boundary (displayed in blue) was sampled near the top of the Mobil San Clemente well (Fig. 1C), where it is within the Capistrano Formation (Rivero and Shaw, 2011) or, consistent with Capistrano Formation, a late Miocene–early Pliocene interval (Crouch and Suppe, 1993). We used independent formation picks (provided by John Shaw, 2014, personal commun.) to test our seismic stratigraphic correlations to two additional southern wells. H4 is near a top Repetto pick in the Shell Oceanside well, and below an upper Repetto pick in the Shell Point Loma well (J. Shaw, 2014, personal commun.). The Repetto Formation ranges between 4.5 and 2.5 Ma in parts of Los Angeles basin, but can be time transgressive (e.g., Blake, 1991), and can be picked differently (Sorlien et al., 2013). We assign H4 an age of 4.5 Ma with qualitative errors possibly exceeding 1 m.y.; it is more likely to be younger than older.

We define the Miocene1 horizon at the Mobil San Clemente 1 well. We used unpublished well logs including lithologic descriptions and a sonic log, and a time-depth chart constructed from the sonic logs, but had no access to paleontology. The Miocene1 reflection at this well is at a measured depth of ~980 m, and near the Rivero and Shaw (2011) top Monterey Formation, or within the time-equivalent late Miocene Capistrano Formation (Walker, 1975). This is above the top of the middle Miocene San Onofre Breccia (Stuart, 1979) at a measured depth of 1430 m. The estimated age for the Miocene1 horizon is thus 8 ± 2 Ma.

Fault and Fold Geometry

The analysis of the digital fault and horizon surfaces provides new insight into the relations between faulting, folding, and deposition through time. We choose to focus on fault systems and on deforming volumes between bounding faults, and use the term fault wedge to describe simultaneously active fault surfaces that intersect at depth (Crowell, 1974; Eusden et al., 2005). Flower structures (Harding, 1985), or palm tree structures (Sylvester, 1988) include nonvertical faults in the shallow subsurface merging into a deeper subvertical strike-slip fault. We use the term fault wedge for faults that display an asymmetric geometry in cross section, and do not necessarily steepen with depth (e.g., Figs. 5 and 6). Deformation within the northern (San Mateo–Carlsbad and Newport–Inglewood) wedge includes contractional folding that deforms the Quaternary top lower Pico and late Quaternary Q unconformities (Figs. 5–9). Faults imaged in Figure 6 discontinuously link the Newport–Inglewood fault southward to the San Mateo–Carlsbad fault, representing internal deformation of the northern fault wedge. The San Mateo–Carlsbad fault steepens south of cross-section 20, where the linking faults have merged with it (Figs. 10 and 11).

Northern Fault Wedge: Oceanside Detachment versus Oceanside Fault Zone

We interpret a gently east-dipping fault beneath and southwest of the San Mateo–Carlsbad fault (Crouch and Suppe, 1993; Bohannon and Geist, 1998). This Oceanside detachment likely accommodated large-scale oblique crustal extension and exhumation of Catalina Schist during Miocene time (Crouch and Suppe, 1993; Nicholson et al., 1993; Bohannon and Geist, 1998). A detachment fault interpretation is supported because tilted blocks are present only above a high-amplitude subhorizontal reflection (Figs. 6 and 7). This reflection is characteristic of rock basement, an interpretation supported by petroleum test wells sampling Catalina Schist at the depths of similar reflectors on the San Pedro shelf and on Lasuen Knoll (Fig. 1). We interpret moderately dipping shallow faults to merge downward into the detachment (Figs. 10 and 11). One of these faults merging downward into part of the detachment was referred to as the Oceanside thrust (Rivero et al., 2000; Rivero and Shaw, 2011).

Although there is agreement on the existence of the Oceanside detachment and its Miocene history as a large-displacement low-angle (oblique) normal fault, interpretations of its post-Miocene activity differ. Fault blocks above the gently east-dipping Oceanside detachment tilted before deposition of the ca. 4.5 Ma H4 horizon, and for the most part do not show further reactivation or deformation (Figs. 6 and 7). We see no evidence for contraction associated with the north-south segment of this fault zone, including no contractional folding in the part of its hanging wall west of the San Mateo–Carlsbad fault. Because of this lack of thrusting and our different geometric interpretation, we define the steeper east-dipping shallow faults as the Oceanside fault zone (red in Fig. 11) and distinguish these faults from the underlying Oceanside detachment (gray in Fig. 11). The Oceanside fault zone and San Mateo–Carlsbad fault bound a southward-widening and deepening triangular basin containing pre-late Pliocene strata as thick as ~4 km (Figs. 6, 7, 10, and 11).

Southern Fault Wedge

Another ~15-km-wide zone of subparallel fault strands between 33°N and the Mexico border narrows at depth, with the outer faults projecting to intersect near 3–4 km depth (Figs. 12–14). This southern fault wedge is geometrically linked to the northern wedge by connecting faults in the shallow subbottom. The Oceanside detachment underlies both wedges, and the shallow wedges also overlap in map view (Figs. 11A and 13–15). We use the name Coronado Bank fault zone (of Legg, 1991) for the several left-stepping en echelon fault strands above and including the Oceanside detachment. The northern and southern wedges, however, present some geometric and kinematic differences. The downdip intersection of east-northeast-dipping and west-southwest-striking faults is much shallower in the southern wedge than

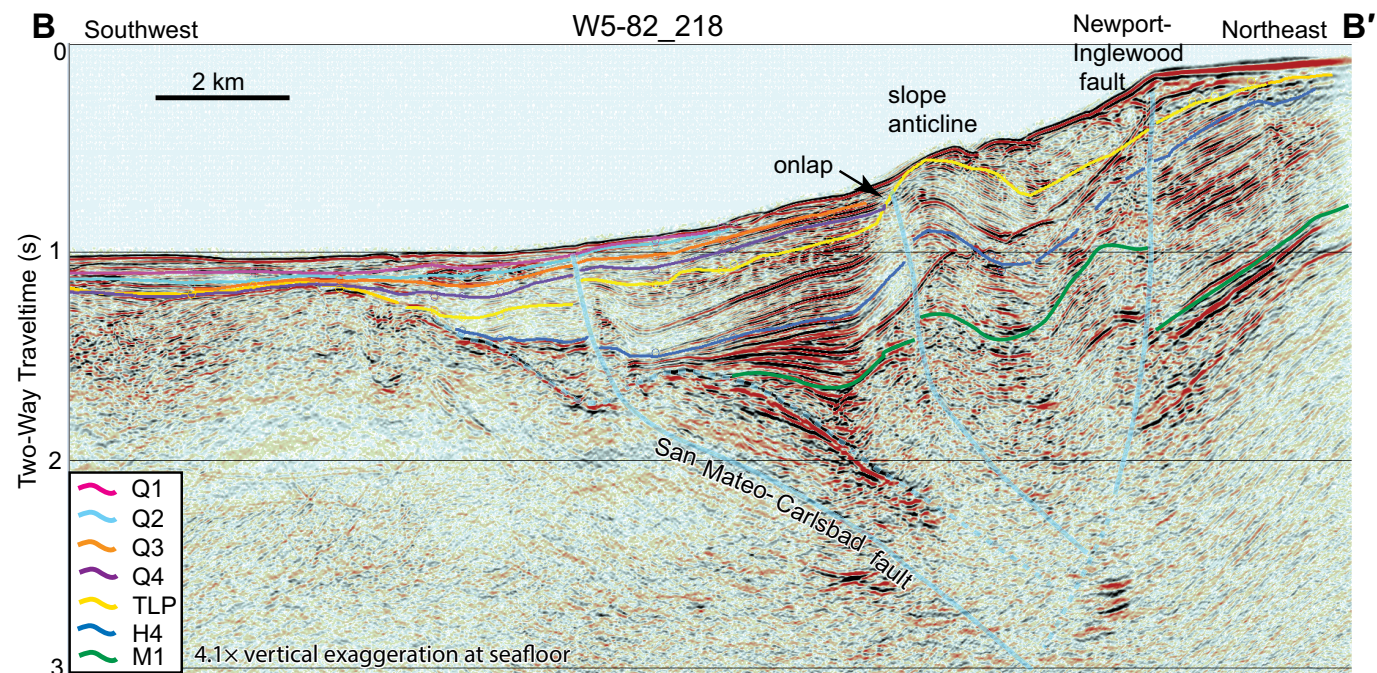


Figure 5. Western Geophysical Company w5-82-218 displayed as profile B-B' (located in Fig. 1; horizons identified in Fig. 2). The San Mateo-Carlsbad fault forms a transpressional fault wedge with the Newport-Inglewood and intervening faults. TLP—top lower Pico. There is no thinning of the section onto the slope anticline below TLP, but much onlap onto TLP. This is consistent with a 1.95 Ma initiation of contractional folding here.

in the northern fault wedge, where it occurs deeper than 8 km (see sections 26–51, Fig. 10). All strands of these southern faults exhibit normal separation for the youngest imaged strata. Furthermore, there is no folding in the south that can be unambiguously interpreted as contraction due to blind (oblique) thrust reactivation.

Stepover Between Wedges and Regional Transtensional Geometry

Figure 14 illustrates a geometry of parallel-striking Miocene faults with tens of kilometers of overlap. North-striking faults link across between north-northwest-striking faults. Furthermore, the linking faults offset Quaternary strata, and the vertical component of the offset across the north-northwest-striking faults changes across the fault intersections. This suggests that there is a transfer of displacement between the overlapping faults, and therefore that the fault geometry is that of a right-releasing stepover rather than of a releasing double bend (e.g., Crowell, 1974).

A 15 km right stepover separates the northern and southern fault wedges, as measured at their downdip bounding fault intersections (Fig. 14). We see no evidence for significant Quaternary shortening south of this stepover. More specifically, Quaternary shortening is not present south of a bend in the San Mateo-Carlsbad fault at lat 33°N and continuing to the west-southwest as far as the Thirtymile Bank detachment (Figs. 1B, 1D). MCS profiles image a dramatic change in Quaternary deformation along the San Mateo-Carlsbad fault as it bends. Reverse separation and contractional hanging-wall folding characterize the northwest-striking fault, with normal separation across the north-striking part of the fault to the south of the bend (Figs. 9–11).

The releasing (transtensional) pattern of north-striking faults is not limited to the bend and stepover between the northern and southern fault wedges. Faults link between the Newport-Inglewood-Rose Canyon fault zone and the Descanso fault (Fig. 14). These faults include the newly mapped west-dipping fault, the Connector fault (Figs. 1 and 14), which has been active in the Quaternary because it offsets the top lower Pico horizon, and the late Quaternary Q4 horizon folds above it. This is the case at least in its northern part, where

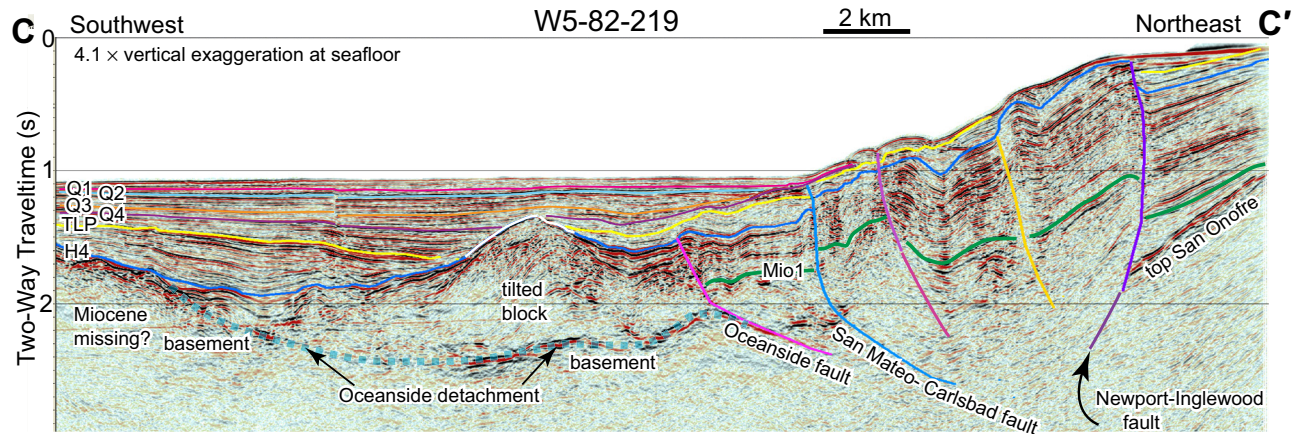


Figure 6. Profile C-C' (location in Fig. 1). The mainly late Miocene interval between horizon Miocene1 (Mio1) and early Pliocene horizon H4 is thickest beneath the modern slope and shelf, above east-northeast-dipping faults. This can be explained by a change of slip direction from transtension to transpression during Quaternary time. The Oceanside detachment (dashed reflection in cyan) underlies the labeled tilted block. Based on correlation 5.5 km along-strike to the Mobil San Clemente 1 well, we interpret the strong labeled reflection northeast of the Newport-Inglewood fault to be the top of the middle Miocene San Onofre Breccia. The shallow basement beneath the southwestern part of the bathymetric basin leaves little room for Miocene strata. Note the nearly undeformed nature of the Q1-Q4 sediments west of the San Mateo-Carlsbad fault, indicating that this shallow portion of the Oceanside detachment is inactive (see Fig. 7). TLP—top lower Pico.

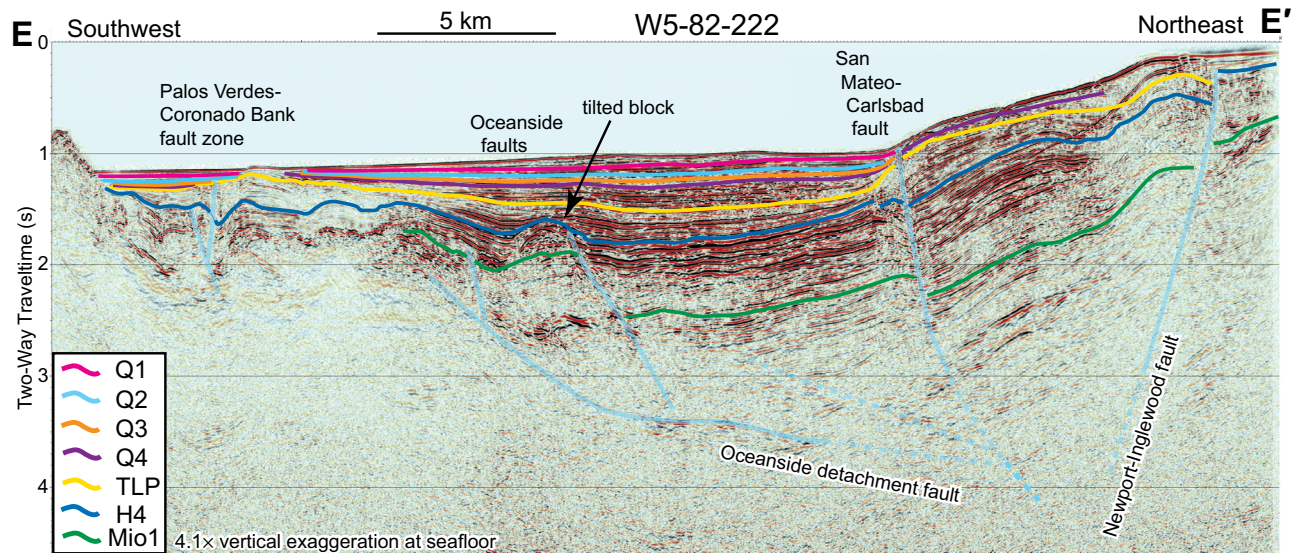


Figure 7. Profile E-E' (location in Fig. 1). This profile is close to a published profile that identified the Oceanside detachment fault (Bohannon and Geist, 1998, Fig. 6 therein). This profile crosses the San Mateo-Carlsbad fault in its more north-south segment (Fig. 1), where structural and bathymetric relief are more subdued than in north-west-striking segments such as on H-H' and G-G' (Figs. 8 and 9). The top lower Pico (TLP) to early Pliocene horizon H4 interval is thicker in the northeast hanging wall of the San Mateo-Carlsbad fault than in its footwall; therefore, transtension continued into early Quaternary time at this location, and was only overprinted by transpression since ca. 2 Ma. Down-to-the-southwest stratigraphic separation across the Newport-Inglewood fault here is opposite to that on C-C', consistent with strike-slip faulting (Fig. 6). Mio1—Miocene1 (late Miocene; see text); TLP—top lower Pico.

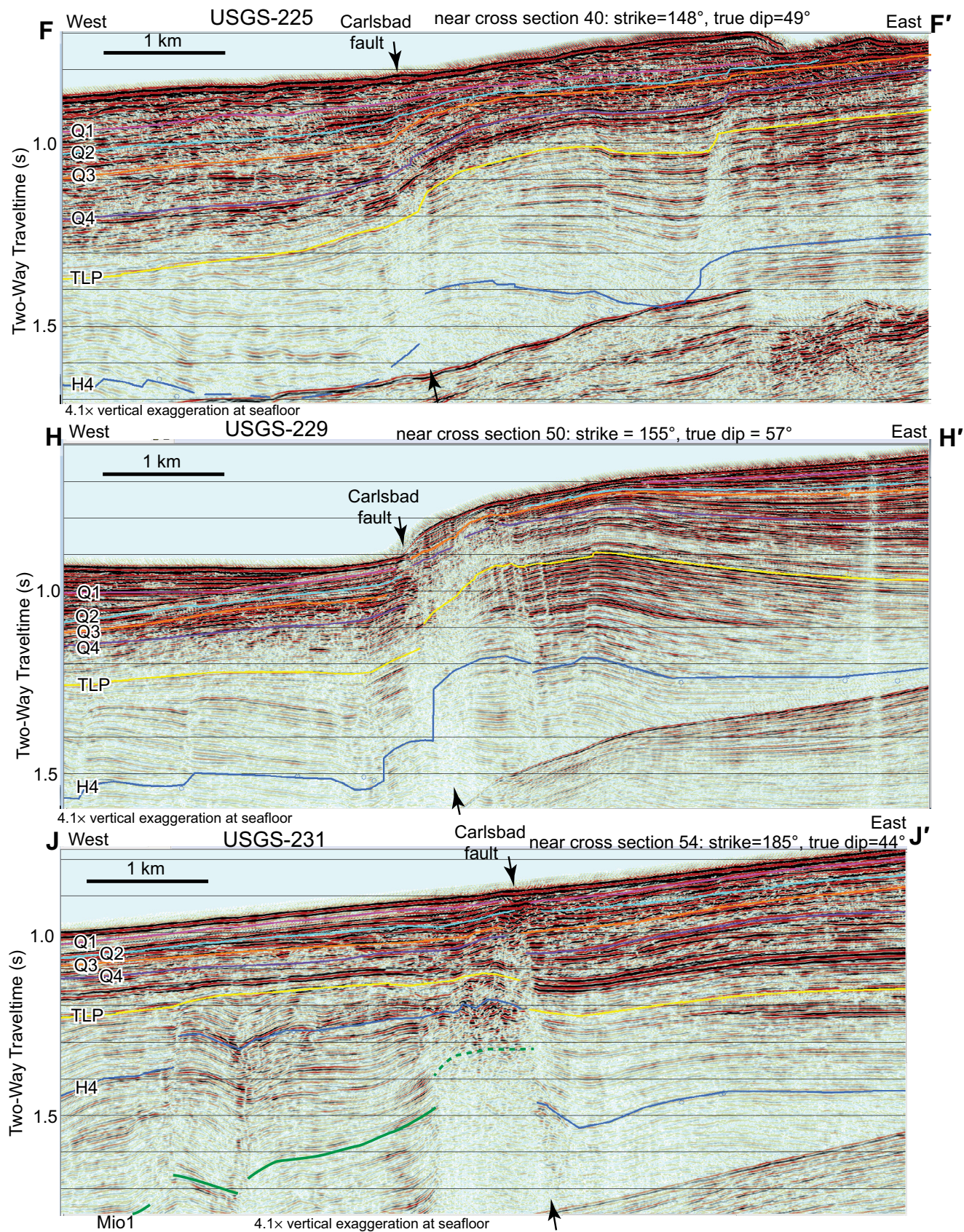


Figure 8. U.S. Geological Survey (USGS) high-resolution multichannel seismic (MCS) reflection profiles showing interpreted stratigraphy across the San Mateo–Carlsbad fault (arrows). Profile locations are in Figure 1. The local strike azimuths and true dips are labeled above each profile: southeast strikes of N148°E and N155°E are restraining and the north-south strike of N185°E is releasing for right-lateral motion, as seen by the reverse component on F–F' and H–H' and the normal separation on J–J'. This changing apparent vertical separation with strike strongly suggests that the principal motion along this part of the San Mateo–Carlsbad fault is right lateral. Profile F–F' (along with other MCS profiles) demonstrates that top lower Pico (TLP) through Q1 horizons can be directly correlated across the fault. These reflections were also correlated on both sides of the fault along numerous MCS profiles of different orientations. Horizon Mio1 (Miocene1) is below the base of the figures except on the west part of J–J'.

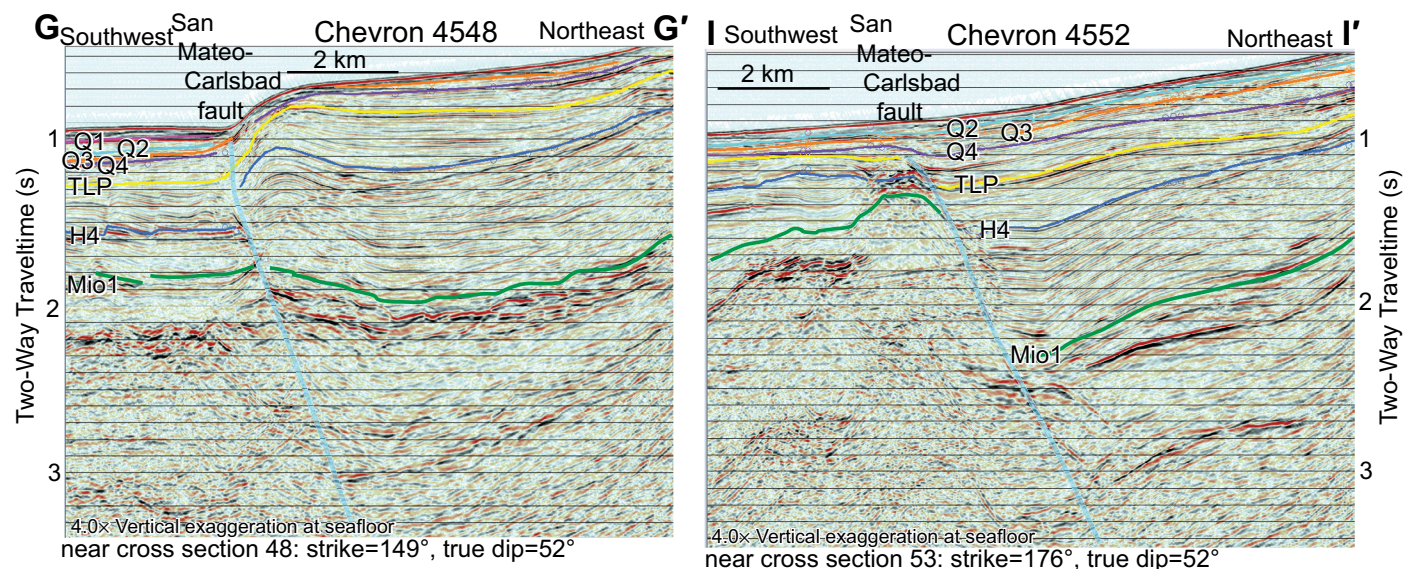


Figure 9. Migrated Chevron profiles located near the northern bend in the major right stepover between the San Mateo–Carlsbad fault and the Descanso and Coronado Bank fault zones. Profile locations are in Figure 1. All interpreted horizons on I–I' exhibit normal separation, just 5 km south of G–G', where they exhibit mostly reverse separation with right-lateral faulting. Note also that ca. 8 Ma horizon Miocene1 (Mio1) on G–G' has no reverse separation while early Pliocene horizon H4 has almost 0.5 km of reverse structural relief near the fault. A Miocene–Pliocene normal component of slip followed by Quaternary reverse separation produced little net relief of Miocene1. TLP—top lower Pico.

these Quaternary horizons have been correlated to and across the fault (below the resolution of cross-sections S1–S3 in Fig. 13). An additional network of north-striking faults through San Diego Bay also connects the Rose Canyon fault to the Descanso fault strands (Kennedy and Weldon, 1980; Kennedy et al., 1980; Jennings and Bryant, 2010).

An unknown amount of inferred right-normal oblique motion on the Connector fault and oblique right-normal slip on San Diego Bay faults, consistent with the estimated ~1.5 mm/yr Holocene right-lateral slip on the Rose Canyon fault (Lindvall and Rockwell, 1995), would enhance the extensional component of the stepover. Thus, one can view the geometry of the southern fault system as a 50-km-long zone of spatially progressive right stepovers and right-releasing segments between the big bend of the San Mateo–Carlsbad fault at 33°N and the offshore Mexico border (Fig. 14). Our detailed mapping documents that the Coronado Bank fault zone is composed of an echelon, nearly north-south fault strands (a releasing geometry in this area) rather than a simple northwest-southeast fault or fault zone, as proposed by Jennings and Bryant (2010) and Rivero and Shaw (2011). The zone of north-striking faults was even longer, 80 km, during late Miocene time, when the Oceanside fault zone and underlying parts of the Oceanside detachment were active.

Sedimentation Through Time

Our sediment isochore (vertical thickness) maps provide a synoptic view of the relationship of sedimentary deposition to fault location, and thus activity, including fault-related folding (Figs. 5–7 and 15). These maps were produced from the depth-converted Miocene1, H4, top lower Pico, Q4, and the seafloor. Miocene sedimentary rocks are thin or missing in the footwall west of the Oceanside fault zone, along the west side of the San Pedro Basin (Figs. 1 and 15). This compares to 1.7 km thickness of Miocene sedimentary rocks sampled in the Mobil San Clemente well, which bottomed in Miocene San Onofre Breccia. Models for tectonic denudation of Catalina Schist in the Inner Borderland predict Miocene sedimentary and volcanic rocks immediately above the schist (Yeats, 1976; Crouch and Suppe, 1993). If that is the case, 4–5 km of Miocene rocks overlie deeper parts of the Oceanside detachment (Fig. 10). Alternatively, pre-Miocene forearc sedimentary rocks could be part of that thickness (Crouch and Suppe, 1993).

The ca. 8–4.5 Ma interval displays substantial thickening in the hanging wall above (east of) the north-south Oceanside fault system and east-northeast of the San Mateo–Carlsbad fault (Fig. 15). Less pronounced thickening into the hanging wall of the San Mateo–Carlsbad fault continues in the ca. 4.5–2 Ma

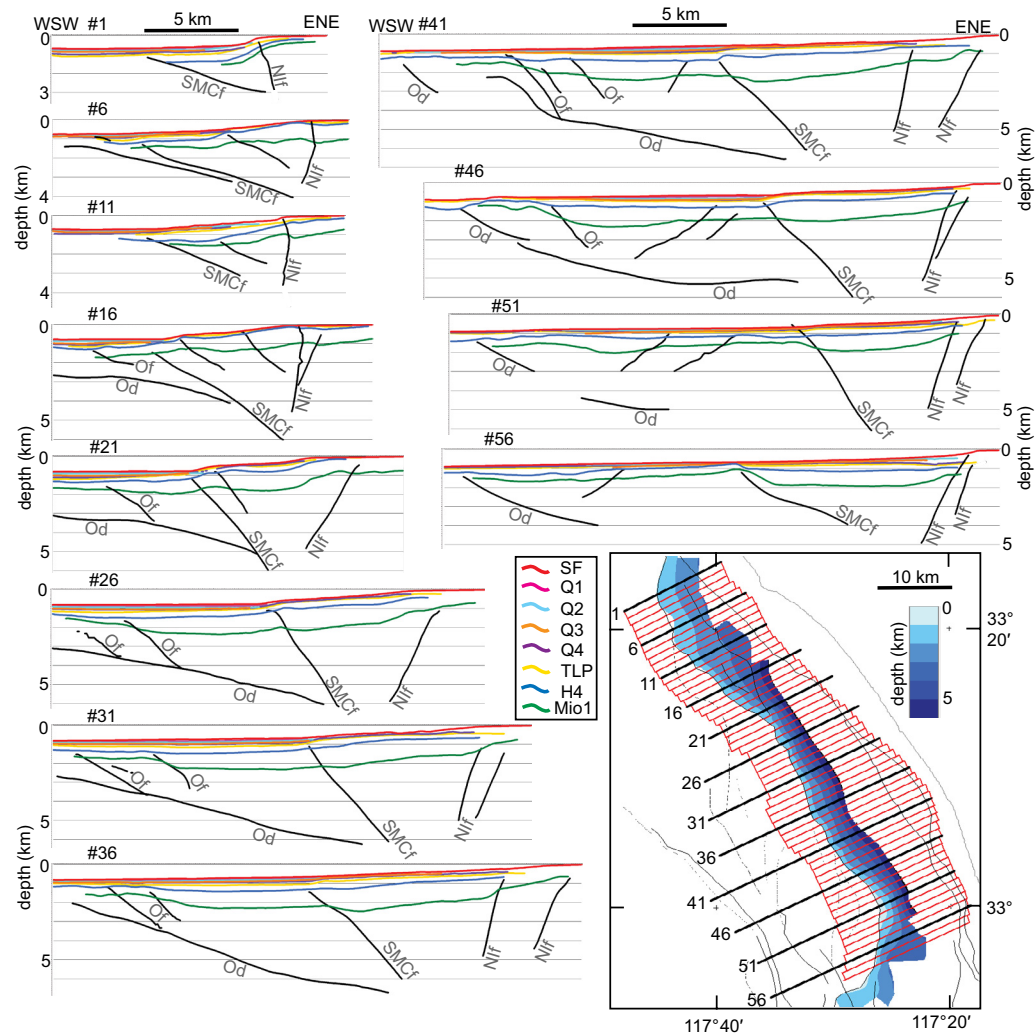


Figure 10. Every fifth cross section from the 58 sections through our depth-converted stratigraphic grids and faults is displayed here with no vertical exaggeration; these sections are numbered and highlighted in black in the inset map. The inset map locates all 58 sections in red, spaced at 1 km, that were used for strike, dip, and structural relief measurements. The depth-converted San Mateo-Carlsbad fault surface and traces of other faults are also on the map. SF—seafloor, TLP—top lower Pico, Mio1—Miocene1; the stratigraphy is identified in Figure 2. Faults: Od—Oceanside detachment; NIf—Newport-Inglewood fault; Of—Oceanside fault; SMCf—San Mateo-Carlsbad fault.

interval, while the Oceanside fault system does not seem to significantly affect deposition during that time range. The ca. 2–0.6 Ma deposition pattern is little affected by faulting or by fault-related folding and tilting, except in the north-south-releasing segment of the southern San Mateo-Carlsbad fault. Sedimentation rates during that time interval appear much slower than for the intervals before and after; this implies either a slower supply of sediment, or sediment bypass through the interpreted area (e.g., Normark et al., 2009). The most dramatic pattern on the ca. 0.6 Ma to present interval is thick deposition in the western footwall and thin deposition in the eastern hanging wall of the

San Mateo-Carlsbad fault. The MCS data image the seafloor to be subparallel to the top lower Pico horizon (Figs. 5–7), with much of the structural relief on at least part of that fault postdating the ca. 0.6 Ma deposition of Q4 (Figs. 8, 9, and 16). Most of the relief of the narrow seafloor slope between the modern continental shelf and the San Pedro Basin thus postdates 0.6 Ma. The late Quaternary reverse component of displacement on San Mateo-Carlsbad fault has been partially blind, and was accommodated by fault-related folding. The Miocene-Pliocene basin in its hanging wall therefore was inverted mainly during late Quaternary time (Fig. 15).

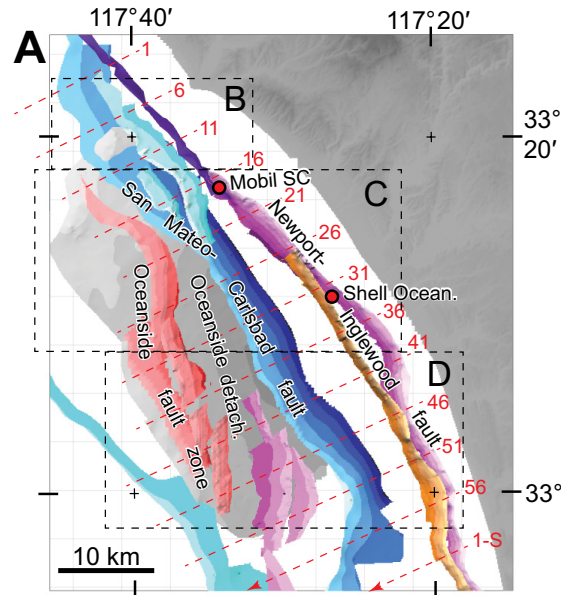
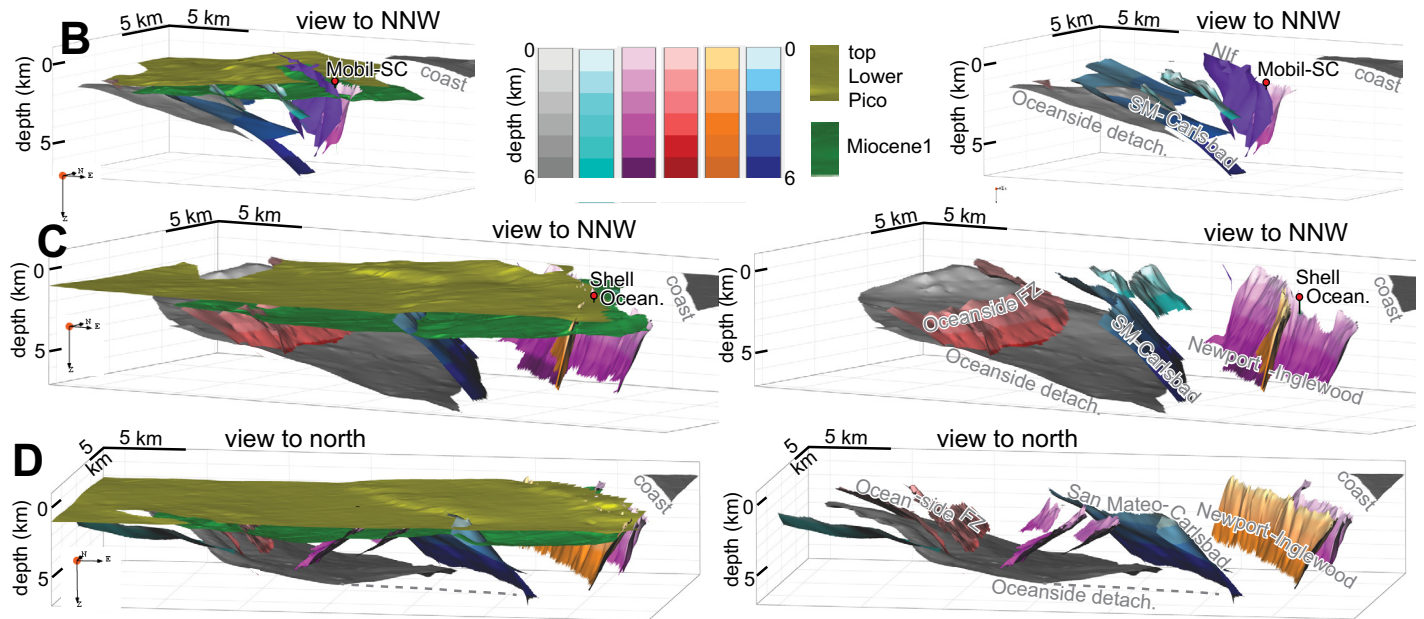


Figure 11. (A) Map view of faults, including those with little evidence of Quaternary activity. Color shading changes every 1 km of depth. The northern part of the Newport-Inglewood fault has a complex shape (passing through vertical), so it is displayed as a single shade of purple. Dashed rectangles show the locations of the B–D volumes. Numbered dashed red lines correspond to the cross sections in Figure 10. The left sides of B, C, and D also include the top lower Pico (TLP, ca. 1.95 Ma) and Miocene1 (ca. 8 Ma) horizons; the right side gives the same volume and same view angle displaying only faults. Roughness and wrinkles are artifacts of gridding; the dense distribution of seismic reflection profiles means that kilometer-scale features are real. (B) Oblique view to north-northwest displayed in depth, with no vertical exaggeration. Broad folding of TLP above this gently dipping part of the San Mateo–Carlsbad fault (blue) implies a post–2 Ma thrust component of slip. The Oceanside detachment (detach., gray) is interpreted on top of a basement reflection known to be the Catalina Schist in wells 50 km to the northwest and well 311 #1 on Lasuen Knoll, 30 km to the west-northwest (location in Figs. 1C, 1D; see text). (C, D) Oblique views to the north-northwest and north, respectively. Strands of the Oceanside fault zone (reds) are interpreted to truncate downward into the Oceanside detachment (grays). The Miocene1 to TLP thickens eastward across the Oceanside fault zone, but there is no evident deformation of the TLP across this zone or above this part of the Oceanside detachment. Steeply dipping Newport–Inglewood strands (magentas and oranges) project toward the other faults, forming one side of this asymmetric fault wedge.



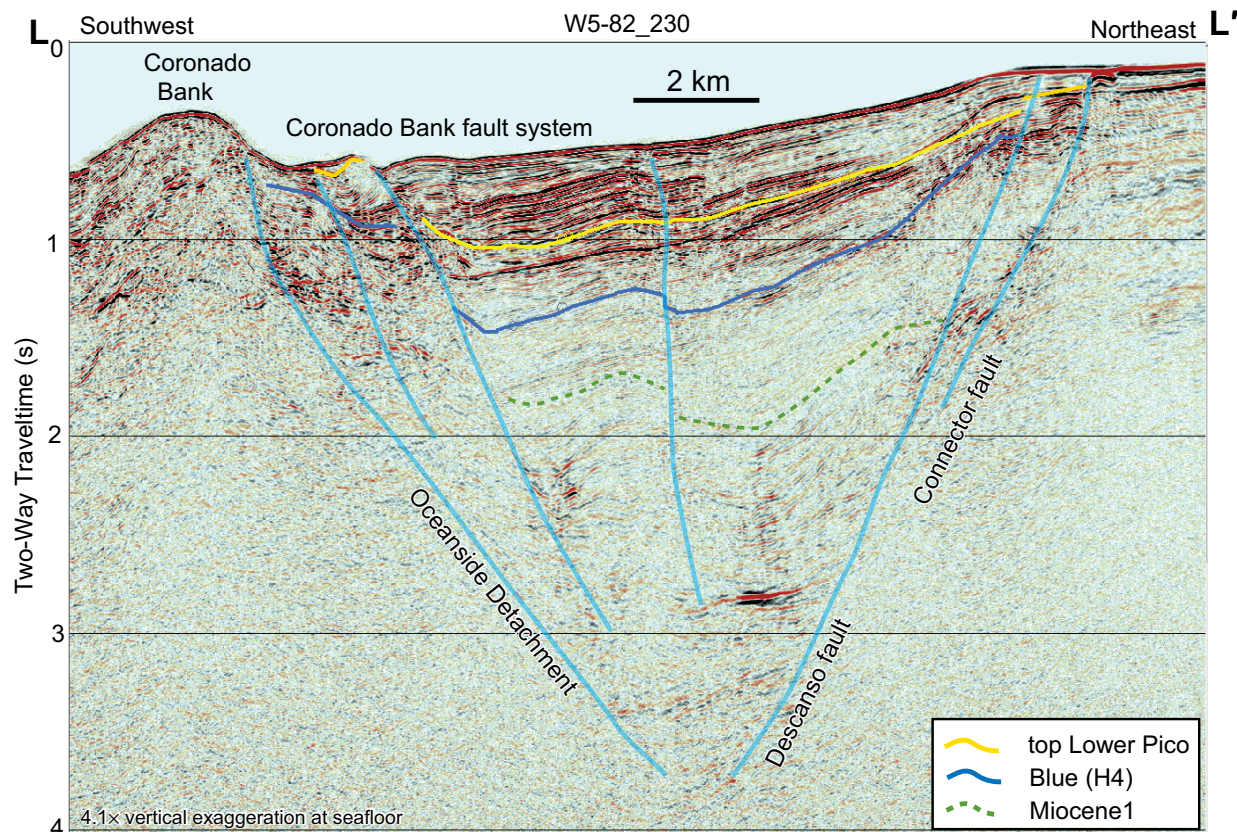


Figure 12. Western Geophysical Company profile L-L' (location in Fig. 1). Fault wedge geometry is imaged adjacent to San Diego. The ca. 2 Ma top lower Pico horizon and strata above it display normal separation across faults.

Kinematic Modeling

The structural relief due to faulting and folding of the top lower Pico is closely associated with the changing strike of the San Mateo–Carlsbad fault (Fig. 16). Northwest-striking parts of the fault have the largest reverse (positive) structural relief, while north-striking fault segments display normal (negative) relief (south) or little relief (north). This systematic pattern can be explained by a right-lateral component of average displacement on the fault. To quantitatively test this hypothesis, we modeled the vertical relief that would be produced along the San Mateo–Carlsbad fault for a range of cumulative displacements and a range of displacement directions, using the approach described herein (Estimating Fault Displacement). Model curves were then

qualitatively compared to the measured structural relief of the ~1.95 top lower Pico horizon to estimate the best match for different displacement directions at different parts of the fault (Fig. 17).

There is no single displacement direction and magnitude that produces a close match along the entire modeled 58 km of the fault. We therefore examine displacement directions that match a given magnitude of modeled displacement for different segments of the fault. Thus, reverse or oblique-right reverse displacement match best in the north-northwest, oblique reverse right lateral matches best in the center, and right lateral matches best in the south-southeast. Use of Equation 4 converts the 0.5–0.8 km range of horizontal hanging-wall displacement that can be read from Figure 17C to 0.6–1.0 km of true oblique displacement along the fault surface. The large change in

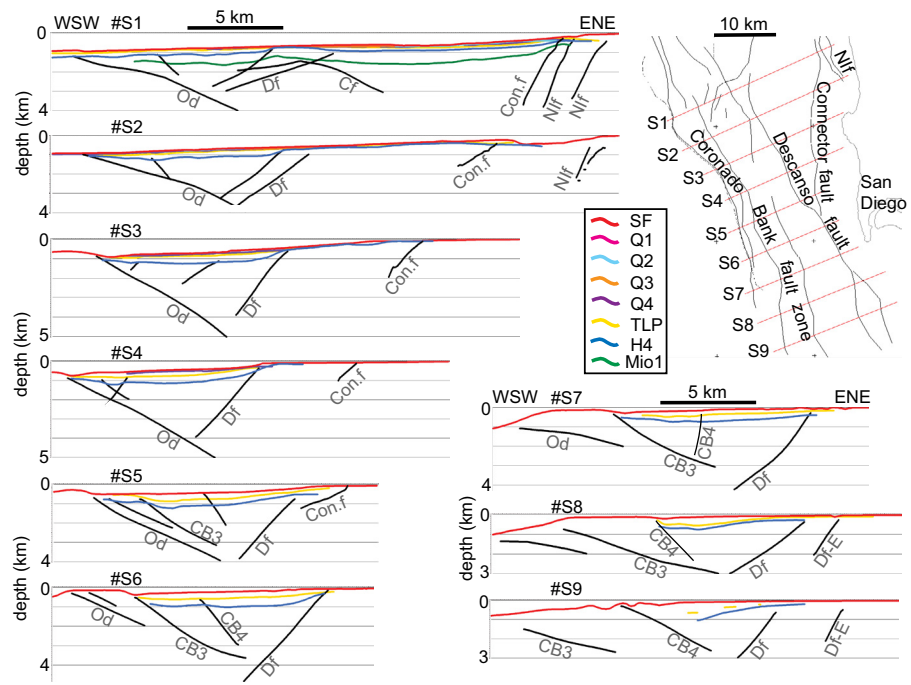
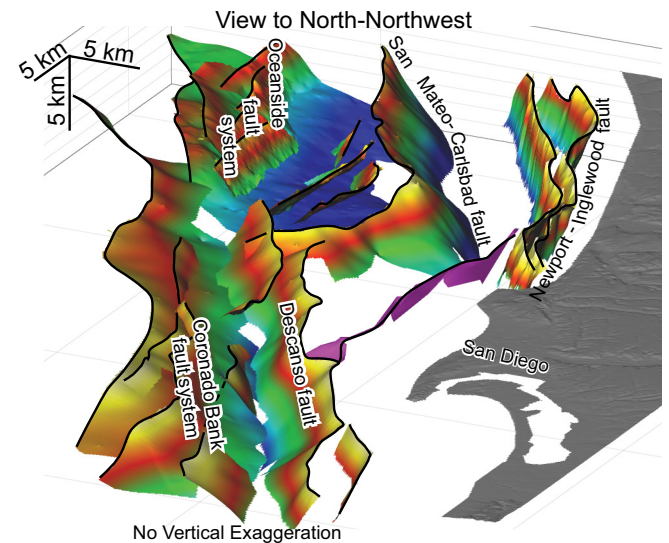
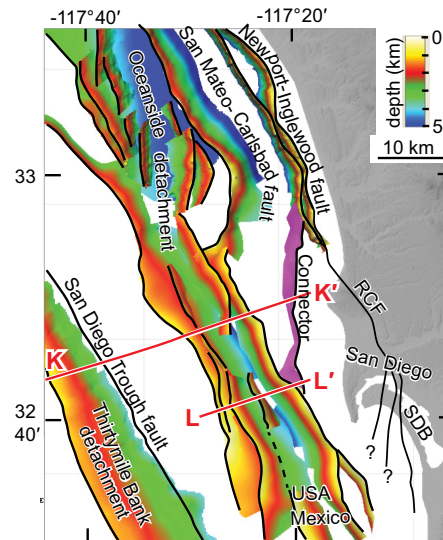


Figure 13. Cross sections with no vertical exaggeration across faults located south of the major right stepover, offshore San Diego. Sections are located on map at upper right. Horizons are seafloor (red, SF), top lower Pico (yellow, TLP), H4 (blue), and Miocene1 (green, Mio1). The late Quaternary Q4 is on S1–S3; Q2 and Q3 are only interpreted on the northern section. Od—Oceanside detachment, CB3 and CB4—Coronado Bank splay 3 and 4, Cf—San Mateo–Carlsbad fault, Df—Descanso fault, Df-E—eastern splay Descanso fault, Con.f—Connector fault, Nif—Newport-Inglewood fault.

Figure 14. Right: An oblique view to the north-northwest of depth-converted fault surfaces, displayed with no vertical exaggeration. This perspective illustrates the overlap between the northern and southern fault wedges and the series of north-striking linking faults between them. The southern faults display a left-stepping in echelon pattern. Left: The same volume, displaying faults in plan view. Several faults are shown only as upper traces. Figures 10 and 13 show the geometry of faults in cross section. Some of the faults continue beyond where mapped into Mexico waters. RCF—Rose Canyon fault; SDB—San Diego Bay.



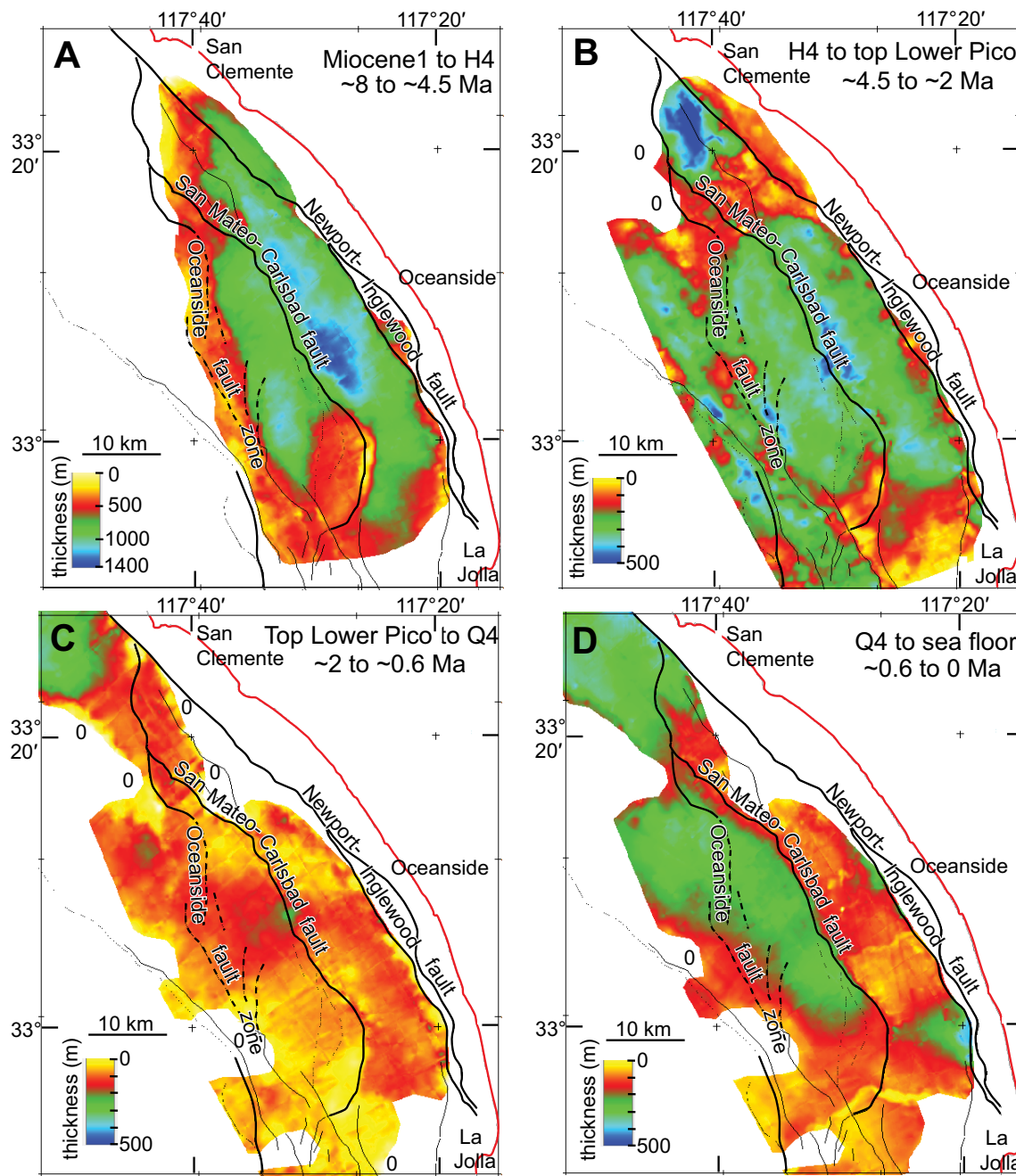


Figure 15. (A-D) Isochore (vertical thickness) maps constructed from the interpreted horizons labeled at the top of each panel (location in Fig. 1A). Upper left in A has a different thickness range for the color scale; B-D have the same range. White is not interpreted, and need not be thin; a few points with zero depositional thickness for each interval are labeled 0 by examination of seismic reflection profiles. Faults from Figure 1 are shown; Miocene faults from Figure 11 are shown as dotted lines. The west side of the late Miocene basin in A is not laterally offset by the San Mateo-Carlsbad and Newport-Inglewood faults. Focusing of deposition into the modern depositional basin west-southwest of the San Mateo-Carlsbad fault is not seen until the 0.6 Ma to present interval in D.

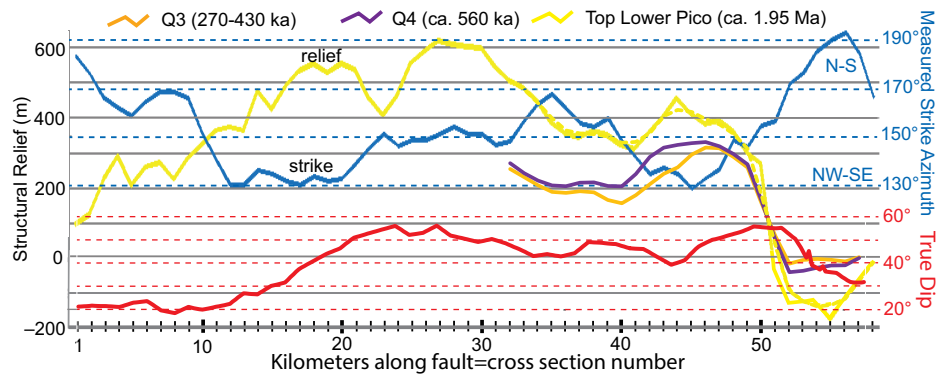
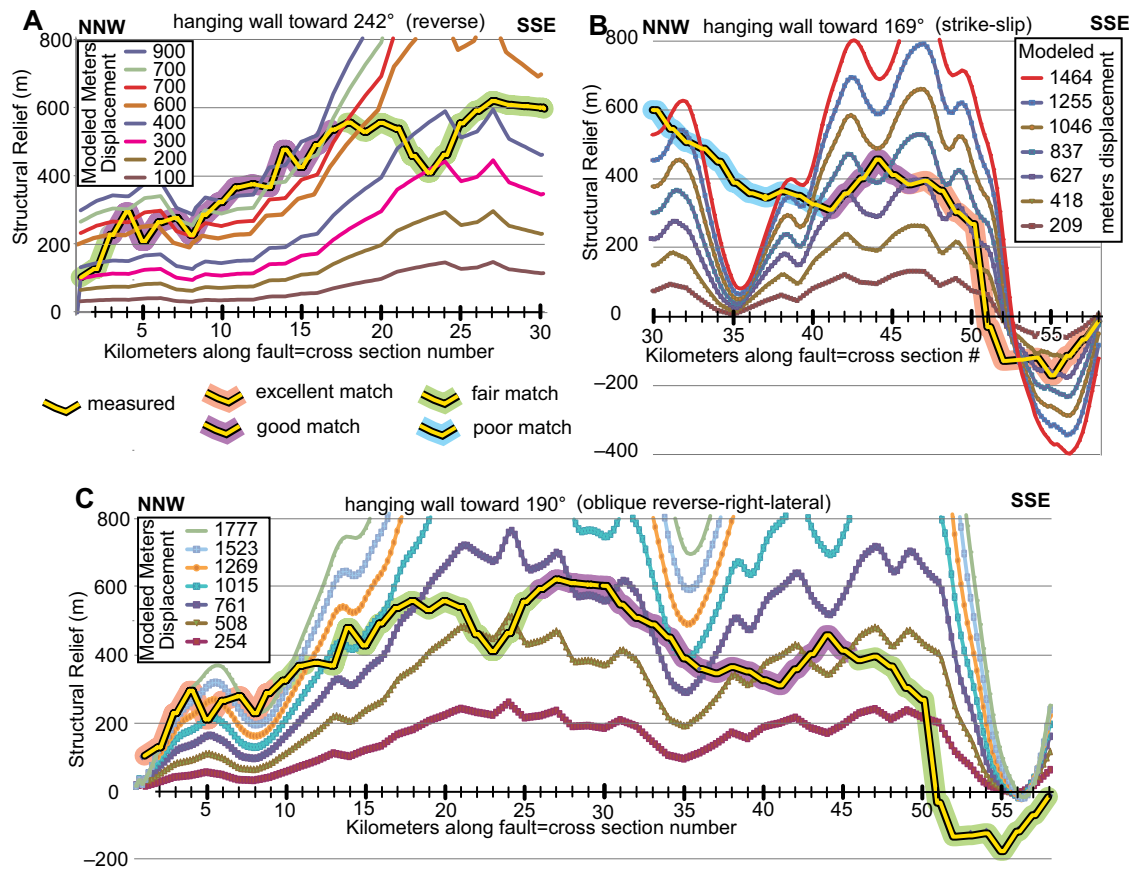


Figure 16. A line graph illustrating the relationship between San Mateo–Carlsbad fault smoothed strike in azimuth degrees (blue), true dip (red), and measured top lower Pico (TLP) structural relief (yellow). Numbers along the horizontal axis, labeled in kilometers along strike, also refer to the individual cross section labeled in Figure 10. Positive (reverse separation) TLP structural relief is measured between km 1 and 50. TLP relief is negative (normal separation) between km 51 and 58. Northwest strikes are associated with the largest contractional (positive) relief, while north strikes are associated with extensional (negative) structural relief. Steeper dip is also associated with larger structural relief. Q3 (orange), Q4 (violet) and TLP (dashed yellow) are displayed between km 32 and 57. The relief pattern between TLP and Q4 is similar, suggesting only a slight rotation of displacement direction through Quaternary time.

Figure 17. Graphs comparing the horizontal component of motion of the hanging wall block with respect to the footwall block of the San Mateo–Carlsbad fault and measured top lower Pico structural relief. Numbers along the horizontal axis, labeled in kilometers along strike, also refer to the individual cross section labeled in Figure 10. Figure 16 gives the strike and dip of the fault, also using the same distance along the fault scale. Equation 4 (see text) permits conversion of the horizontal component of displacement to true displacement on the fault. Azimuths 242°, 169°, and 190° (clockwise from north) represent reverse, right-lateral, and oblique reverse right-lateral motion, respectively. The color of the thick background shading gives our qualitative opinion of the curve matching for different parts of the fault, for a consistent magnitude of horizontal fault displacement.



displacement azimuth along the fault implies clockwise vertical-axis rotation of the footwall (west) with respect to the footwall (also suggested by Ryan et al., 2009), and/or a transfer of right-lateral motion from the Newport-Inglewood fault southward to the San Mateo–Carlsbad fault through a deforming fault wedge (see Conrad et al., 2014).

In order to test whether the late Quaternary deformation pattern is similar to that reflected by the deeper top lower Pico horizon, we also measured structural relief of the Q horizons. Although part of this relief could be due to initial vertical position at the time of deposition (seafloor relief), the top lower Pico to Q4 thickness map in Figure 15 indicates little effect on sedimentation by the San Mateo–Carlsbad fault, suggesting gentle seafloor paleoslope near this fault's trace. Variations in structural relief of the top lower Pico, Q4 (ca. 560 ka), and Q3 (ca. 430–270 ka) are plotted against fault strike along 25 km of the fault (Fig. 16). A similar spatial pattern of structural relief between these three horizons indicates that the average ca. 1.95 Ma to present fault displacement that we modeled continued through the ca. 560 ka to present interval. The 60 m right offset or deflection of submarine ravines at the slope-basin transition near the San Mateo–Carlsbad fault (Conrad et al., 2014) supports continued late Quaternary activity. Right-lateral deformation has also been proposed for this fault system based on high-resolution seismic reflection data (Bormann et al., 2014).

■ DISCUSSION

Careful interpretation and analysis of faults and stratigraphic reference horizons in 3D reveal important details of offshore deformation that differ significantly from some previously proposed models. These details concern (1) the age of stratigraphic units; (2) the relation of geometry and continuity of faults to structural relief, basin development, and style of faulting; (3) the relations of fault geometry during the change from transtension to transpression to whether faults are abandoned or continue activity; and (4) the degree of strain partitioning or strain localization among the various faults accommodating the observed oblique crustal deformation. All of these elements bear directly on the inferred seismic hazard and tsunami potential of these active offshore structures and the risk they pose to coastal communities in southern California.

Continuity of Faulting from Geometry, Sedimentation, and Kinematics

Our results suggest that the San Mateo–Carlsbad fault is geometrically continuous (Fig. 1), much more so than previously interpreted (Ryan et al., 2009; Jennings and Bryant, 2010). Late Miocene through late Quaternary depositional thickness changes are strongly associated with the position of the San Mateo–Carlsbad fault and the folding above it, supporting our interpretation of a single throughgoing fault (Fig. 15). Our kinematic modeling of between

0.6 and 1.0 km of true fault slip also implies continuity, despite gradual spatial changes in displacement direction.

The overlapping Newport-Inglewood fault strands also are part of a continuous fault zone that strikes southward to connect with the onshore Rose Canyon fault in San Diego (Fig. 11). Others have mapped discontinuous segments of this fault zone with gaps (e.g., Jennings and Bryant, 2010). Both Ryan et al. (2009) and Jennings and Bryant (2010) interpreted a gap in the Newport-Inglewood fault near Dana Point (DP in Fig. 1B). We interpret instead a continuous offshore Newport-Inglewood fault at this location and others for the following reasons. First, a southwest-dipping reflector interpreted as a thrust by Rivero and Shaw (2011) near the top of San Onofre Breccia is in fact offset by the Newport-Inglewood fault (just below the green Miocene 1 horizon in Figs. 5–7, labeled top San Onofre in Fig. 6). Second, the Dana Point area is where the Newport-Inglewood fault transitions from being a clearly imaged fault on the shelf (e.g., B–B' in Fig. 5) to changing character as it cuts across the slope in an area where steep stratal dip degrades imaging, thus resulting in an apparent fault gap.

Kinematics and Evolution

Major early and middle Miocene oblique extension along the Inner California Continental Borderland is well documented. For example, tectonic denudation of Catalina Schist and deposition of schist fragments in the middle Miocene San Onofre Breccia require such extension, and the associated faults are imaged (Yeats, 1976; Crouch and Suppe, 1993; Bohannon and Geist, 1998). How, when, and where continuing late Miocene extension has or has not been overprinted by subsequent transpression, or whether there are locations where extension continued into Pliocene or Quaternary time, is less well known. Changes in late Miocene sedimentary rock thickness across the Oceanside fault zone and the San Mateo–Carlsbad fault demonstrate an extensional component of fault activity during that time interval, and probably similar motion before ca. 8 Ma. Late Miocene activity on the Newport-Inglewood faults is indicated by progressive tilting in its hanging wall (cross-section S-1 in Fig. 13).

Tectonic models for the oblique opening of the Inner Borderland and denudation of Catalina Schist include faults with at least tens of kilometers of (oblique) normal displacement (Yeats, 1976; Stuart, 1979; Crouch and Suppe, 1993; Nicholson et al., 1994; Bohannon and Geist, 1998; ten Brink et al., 2000; Legg et al., 2004). It does not make kinematic sense that a gently dipping fault with tens of kilometers of displacement could terminate against a strike-slip fault, the Newport-Inglewood fault, which may only have a few kilometers of right-lateral motion (Fischer and Mills, 1991). Even if cut and offset by the Newport-Inglewood fault, the Oceanside detachment likely extends beneath the mainland coastal facilities and small cities. The San Mateo–Carlsbad fault may merge downward with the deep part of the Oceanside detachment, although this relationship is not clearly imaged. The geometric relationship between the Newport-Inglewood fault and San Mateo–Carlsbad fault also is not known (see Rivero et al., 2000). The regional dip between the basin and shelf is not

easily explained by folding related to the Newport-Inglewood fault because both sides of this fault are high standing. The basin-shelf structural relief is more easily explained as a broad forelimb above the San Mateo–Carlsbad fault (our hypothesis), or as a backlimb above the southwest-dipping roof thrust of a southwest-verging wedge (Rivero and Shaw, 2011). While we point out this logic, whether the Oceanside detachment that likely exists beneath the mainland coast has been reactivated as an oblique thrust is beyond the scope of this paper.

There is no significant deformation evident on seismic reflection profiles above the Oceanside detachment, including north-striking strands of the Oceanside fault zone, west of the San Mateo–Carlsbad fault after deposition of the ca. 4.5 Ma H4 horizon (Figs. 6 and 7). This upper, northwestern part of the Oceanside detachment and splays above it were therefore abandoned during early Pliocene time. The San Mateo–Carlsbad fault continued activity during Pliocene through late Quaternary time. Steep strands of the Newport-Inglewood fault also continued activity through Pliocene and Quaternary time.

Regional shortening initiated about the beginning of Pliocene time from offshore south-central California through the Santa Barbara Channel, Santa Monica Bay, and northern Los Angeles basin (Clark et al., 1991; Sorlien et al., 1999, 2006; Seeber and Sorlien, 2000; Willingham et al., 2013; Wright, 1991; Schneider et al., 1996). However, contractional folding did not start on the offshore the San Pedro shelf and escarpment until about the beginning of Quaternary time (Sorlien et al., 2013). Shortening in the part of the Outer California Continental Borderland west to southwest of San Clemente Island initiated at 3.7 Ma (De Hoogh, 2012). Distributed transtensional faults offshore Oceanside were abandoned by 1.95 Ma, with many becoming inactive earlier, perhaps at the beginning of the Quaternary (2.6 Ma; F–F' in Fig. 8). While there is evidence for transpression starting ca. 2 Ma, a major change in sedimentation related to contractional folding and tilting did not occur at this latitude until after formation of the Q4 unconformity, ca. 0.6 Ma. Because we did not interpret stratigraphic reflectors between ca. 2 and 0.6 Ma, it is possible that this major change in sedimentation started before 0.6 Ma. Thus, there appears to have been a spatial progression from north to south, and possibly from west to east, of the change from transtension to transpression along the southern California margin.

The evolution of these fault systems mirrors the Neogene evolution of the Pacific North American plate margin. After early Miocene cessation of microplate subduction, the Pacific plate continued to diverge from the North American plate. Gradual changes in Pacific plate motion through late Miocene time decreased this divergence (e.g., Atwater and Stock, 1998). Transfer of the majority of plate boundary motion into the Gulf of California ca. 6 Ma initiated rapid slip on the southern San Andreas and created its Mojave restraining segment (Crowell, 1979). This reorganization initiated oblique contraction across the western Transverse Ranges (Atwater, 1989) at about the time that the north-striking Oceanside fault zone decreased, then ceased activity. Additional reorganization of the southern San Andreas fault, including initiation of the Elsinore fault at 1.2 Ma (Dorsey et al., 2012), is synchronous with early Quaternary initiation of localized transpression on the San Mateo–Carlsbad fault,

and then late Quaternary basin inversion. Because the northern fault wedge has been continuously active since before ca. 8 Ma, initiation of local transpression followed by basin inversion may represent a change in slip direction rather than reactivation of an abandoned fault.

Modeling of Quaternary displacement for different strikes and dips of the San Mateo–Carlsbad fault and comparison of deformation of older and younger strata allow inferences to be made about the strain on other faults. Transpression, and certainly thrusting, are not expected on north-striking faults, given the strain field we have documented nearby.

Oblique Thrust Reactivation of Regional Gently Dipping Faults

A >200-km-long linked system of low-angle (oblique) normal faults, including the Santa Monica Bay detachment, Catalina Island detachment, and the Thirtymile Bank detachment, dips toward the mainland coast (Figs. 1 and 18) (Sorlien et al., 2013). This fault system, along with the gently east-dipping Oceanside detachment above it, have been interpreted to be active Quaternary thrust faults (Rivero et al., 2000; Rivero and Shaw, 2011). Both these systems extend much farther south into Mexican waters (Legg, 1985, 1991), raising concerns about potential 200+ km thrust ruptures. However, several observations suggest that this scenario is unlikely. The ~15 km right stepover between the northern and southern wedges near 33°N (Figs. 1 and 14) marks an east-north-east–west-southwest limit between Quaternary transpression (north) and transtension (south). This limit includes the San Diego Trough above the Thirtymile Bank detachment (Fig. 1). There is no evidence for Quaternary shortening south of that line and east of the Thirtymile Bank detachment, although MCS reflection data are not available beyond a few kilometers south of the Mexico border. In addition, the more steeply dipping San Mateo–Carlsbad fault and the Newport-Inglewood fault are projected to intersect, interact, and potentially segment these more gently dipping structures at depth. Thus, either there is little thrust hazard on or above the Thirtymile Bank detachment south of lat 33°, or thrusting is too young and/or too slow to have developed significant structure. North of lat 33°, with the exception of the 70-km-long Palos Verdes anticlinorium, shallow thrust reactivation of the >200-km-long series of low-angle normal faults seems to be localized near seafloor knolls, and may be associated with bends in local strike-slip faults, especially the San Pedro Basin fault (Ryan et al., 2012; Sorlien et al., 2013). Therefore, 200-km-long thrust ruptures on any of these systems, with large associated tsunamis, seem improbable.

CONCLUSIONS

An asymmetric fault wedge bounded by the Newport-Inglewood and San Mateo–Carlsbad faults overlies two structural levels of gently landward-dipping faults. The fault wedge has been active since at least

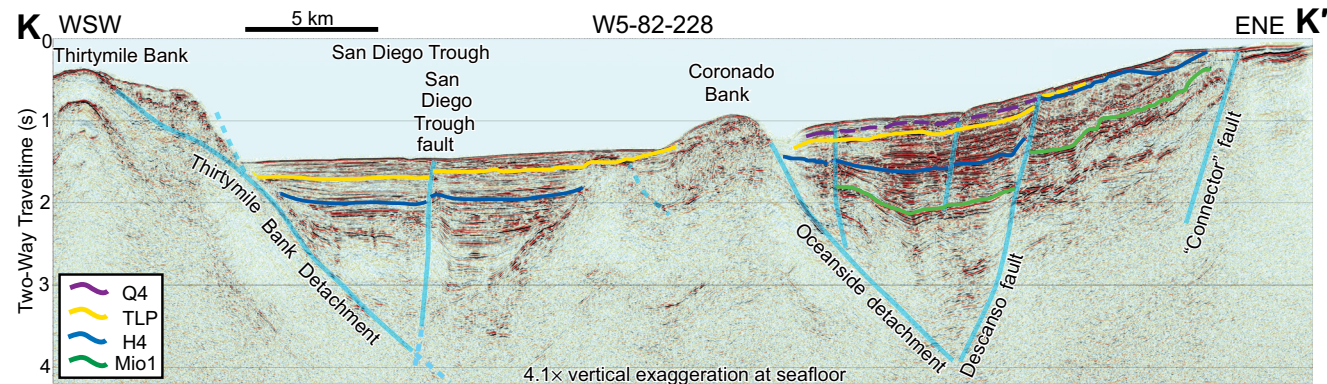


Figure 18. Western Geophysical Company profile displayed as K-K' (location in Fig. 1). Coronado Bank is the upper tip of a tilted block above the Thirtymile Bank detachment. There is no clear evidence for shortening on this profile. The San Diego Trough fault is known to be right lateral during Holocene time (Ryan et al., 2012), while significant Pliocene–Quaternary right-lateral components of slip can be inferred on the Descanso and Connector (see text) faults. Stratigraphic interpretation of San Diego Trough is modified from Alward et al. (2009). TLP—top lower Pico.

ca. 8 Ma. Oblique reverse right-lateral deformation on the San Mateo–Carlsbad fault initiated ca. 2 Ma, after earlier transtension, and before basin inversion above this moderately dipping fault occurred during late Quaternary time (post–780 ka). Cumulative true displacement on the surface of the moderately dipping central and southern parts of this fault has been between 0.6 and 1.0 km during the past 2 m.y., with slip direction varying along strike from thrust or oblique in the northwest, to oblique reverse right lateral, to right lateral and oblique normal right lateral through a bend in the southeast.

The gently dipping faults were (oblique) normal faults with sufficient displacement to expose the Catalina Schist during Miocene time. The shallower system is the Oceanside detachment and fault zone. The Oceanside fault zone ceased significant activity during early Pliocene time. Quaternary deformation focused on fewer and steeper north-northwest–striking faults such as the San Mateo–Carlsbad and Newport–Inglewood with modeled or inferred oblique slip and right-lateral slip. These steeper faults project to intersect the underlying Oceanside detachment and segment it and/or affect its activity landward of the intersections.

A 15 km right-stepover is present between a northern and a southern fault wedge. This stepover is part of a 50-km-long domain of north-striking faults. There is no significant evidence for Quaternary shortening in this domain, south of a west-southwest–east-southeast line passing through the northern bend of the stepover at 33°N. This lack of shortening includes the hanging wall of the deeper gently dipping fault, the Thirtymile Bank detachment. Thus, major or great thrust earthquakes are not expected to affect these fault systems between the city of Oceanside and the offshore Mexico border.

ACKNOWLEDGMENTS

Funded by USDI/USGS (U.S. Department of the Interior/U.S. Geological Survey) awards 08HQGR0103 and G12AP20069. We acknowledge IHS for the donation of Kingdom Suite Software, and WesternGeco, Chevron, and the U.S. Geological Survey for providing the seismic reflection data for the purpose of this research. Publicly available well logs were provided by BOEM-BSEE (USDI Bureau of Ocean Energy Management, Bureau of Safety and Environmental Enforcement). Background geologic discussions with Mark Legg (over decades), and Leonardo Seeber are appreciated. John Shaw provided well picks that we used to test our existing regional correlations. Billy Alward did much work loading the seismic reflection data and in interpretation of the adjoining area to the west, including the San Diego Trough. We thank two anonymous reviewers and associate editor Colin Amos for comprehensive reviews that improved the manuscript.

REFERENCES CITED

- Alward, W.S., Sorlien, C.C., Bauer, R.L., and Campbell, B.A., 2009, Mergence of the Palos Verdes, San Pedro Basin, and San Diego Trough fault zones: A 220+ km-long fault system: Southern California Earthquake Center Annual Meeting, Proceedings and Abstracts v. XIX, poster 2-024, p. 263.
- Atwater, T., 1989, Plate tectonic history of the northeast Pacific and western North America, in Winterer, E.L., et al., eds., *The eastern Pacific Ocean and Hawaii*: Boulder, Colorado, Geological Society of America, *Geology of North America*, v. N, p. 21–72.
- Atwater, T., and Stock, J.M., 1998, Pacific–North America plate tectonics of the Neogene southwestern United States: An update: *International Geology Review*, v. 40, p. 375–402, doi:10.1080/00206819809465216.
- Bennett, J.T., 2012, Analysis of Quaternary faults and associated deformation of sedimentary basin fill: Inner Continental Borderland of southern California [M.S. thesis]: Columbia, University of Missouri, 65 p.
- Blake, G.H., 1991, Review of the Neogene biostratigraphy and stratigraphy of the Los Angeles Basin and implications for basin evolution, in Biddle, K.T., ed., *Active margin basins: American Association of Petroleum Geologists Memoir 52*, p. 135–184.
- Bohannon, R.G., and Geist, E.L., 1998, Upper crustal structure and Neogene tectonic development of the California Continental Borderland: *Geological Society of America Bulletin*, v. 110, p. 779–800, doi:10.1130/0016-7606(1998)110<0779:UCSANT>2.3.CO;2.
- Bormann, J.M., Holmes, J.J., Sahakian, V.J., Klotso, S., Kent, G., Driscoll, N.W., Harding, A.J., and Wesnousky, S.G., 2014, Active faulting in the Inner California Borderlands: New constraints

- from high-resolution multichannel seismic reflection data: American Geophysical Union 2014 Fall Meeting, abs. 30549.
- Clark, D.H., Hall, N.T., Hamilton, D.H., and Heck, R.G., 1991, Structural analysis of late Neogene deformation in the central offshore Santa Maria Basin, California: *Journal of Geophysical Research*, v. 96, p. 6435–6457, doi:10.1029/90JB00922.
- Conrad, J.E., Dartnell, P., Sliter, R.W., Ryan, H.F., Maier, K.L., and Brothers, D.S., 2014, Carlsbad, San Onofre, and San Mateo fault zones: Possible right-lateral offset along the slope-basin transition, offshore Southern California: American Geophysical Union 2014 Fall Meeting, abs. 19264.
- Covault, J.A., and Romans, B.W., 2009, Growth patterns of deep-sea fans revisited: Turbidite-system morphology in confined basins, examples from the California Borderland: *Marine Geology*, v. 265, p. 51–66, doi:10.1016/j.margeo.2009.06.016.
- Crouch, J.K., and Suppe, J., 1993, Late Cenozoic tectonic evolution of the Los Angeles basin and inner California borderland: A model for core complex-like crustal extension: *Geological Society of America Bulletin*, v. 105, p. 1415–1434, doi:10.1130/0016-7606(1993)105<1415:LCTEOT>2.3.CO;2.
- Crowell, J.C., 1950, Geology of Hungry Valley area, southern California: *American Association of Petroleum Geologists Bulletin*, v. 36, p. 2021–2025.
- Crowell, J.C., 1974, Origin of late Cenozoic basins in southern California, in Dickinson, W.R., ed., *Tectonics and sedimentation: Society of Economic Paleontologists and Mineralogists Special Publication 22*, p. 190–204, doi:10.2110/pec.74.22.0190.
- Crowell, J.C., 1979, The San Andreas fault system through time: *Journal of the Geological Society of London*, v. 136, p. 293–302, doi:10.1144/gsjgs.136.3.0293.
- Dartnell, P., and Gardner, J.V., 1999, Sea-floor images and data from multibeam surveys in San Francisco Bay, southern California, Hawaii, the Gulf of Mexico, and Lake Tahoe, California-Nevada: U.S. Geological Survey Digital Data Series DDS-55, v. 1.0.
- De Hoogh, G.L., 2012, Structural and stratigraphic evolution of the central and southern outer California Continental Borderland [M.S. thesis]: Long Beach, California State University Long Beach, 66 p.
- Dorsey, R.J., Axen, G.J., Peryam, T.C., and Kairouz, M.E., 2012, Initiation of the southern Elsinore fault at ~1.2 Ma: Evidence from the Fish Creek–Vallecito Basin, southern California: *Tectonics*, v. 31, TC2006, doi:10.1029/2011TC003009.
- Edwards, B.D., Ehman, K.D., Ponti, D.J., Reichard, E.G., Tinsley, J.C., Rosenbauer, R.J., and Land, M., 2009, Stratigraphic controls on saltwater intrusion in the Dominguez Gap area in coastal Los Angeles, in Lee, H.J., and Normark, W.R., eds., *Earth science in the urban ocean: The Southern California Continental Borderland: Geological Society of America Special Paper 454*, p. 375–395, doi:10.1130/2009.2454(5.4).
- Ehman, K.D., and Edwards, B.D., 2014, Sequence stratigraphic framework of upper Pliocene to Holocene sediments of the Los Angeles basin, California: Implications for aquifer architecture: Upland, California, Pacific Section, SEPM (Society for Sedimentary Geology) Book 112, 49 p.
- Eusden, J.D., Jr., Petinga, J.R., and Campbell, J.K., 2005, Structural collapse of a transpressive hanging-wall fault wedge, Charwell region of the Hope fault, South Island, New Zealand: *New Zealand Journal of Geology and Geophysics*, v. 48, p. 295–309, doi:10.1080/00288306.2005.9515116.
- Fischer, P.J., and Mills, G.I., 1991, The offshore Newport–Inglewood–Rose Canyon fault zone, California: Structure, segmentation and tectonics, in Abbott, P.L., and Elliott, W.J., eds., *Environmental perils, San Diego region: San Diego, California, San Diego Association of Geologists*, p. 17–36.
- Fuis, G.S., Scheirer, D.S., Langenheim, V.E., and Kohler, M.D., 2012, A new perspective on the geometry of the San Andreas fault in southern California and its relationship to lithospheric structure: *Seismological Society of America Bulletin*, v. 102, p. 236–251, doi:10.1785/0120110041.
- Görür, N., and Elbek, Ş., 2014, Tectonic events responsible for shaping the Sea of Marmara and its surrounding region: *Geodinamica Acta*, v. 26, p. 1–11, doi:10.1080/09853111.2013.859346.
- Harding, T.P., 1985, Seismic characteristics and identification of negative flower structures, positive flower structures and positive structural inversion: *American Association of Petroleum Geologists Bulletin*, v. 69, p. 582–600.
- Hart, P.E., and Childs, J.R., 2005, National archive of marine seismic surveys (NAMSS): Status report on U.S. Geological Survey program providing access to proprietary data: Eos (Transactions, American Geophysical Union), v. 86, abs. S41A–10, http://walrus.wr.usgs.gov/NAMSS/.
- Hubbard, J., Shaw, J.H., Dolan, J., Pratt, T.L., McAuliffe, L., and Rockwell, T.K., 2014, Structure and seismic hazard of the Ventura Avenue anticline and Ventura fault, California: Prospect for large, multi-segment ruptures in the Western Transverse Ranges: *Seismological Society of America Bulletin*, v. 104, p. 1070–1087, doi:10.1785/0120130125.
- Hughes, D.R., 1985, V w/o T (Velocity without tears): *The Leading Edge*, v. 4, p. 50–52, doi:10.1190/1.1439131.
- Jennings, C.W., and Bryant, W.A., 2010, California Geological Survey 150th Anniversary fault activity map of California: California Geological Survey Geologic Data Map no. 6, scale 1:750,000, http://www.consrv.ca.gov/cgs/cgs_history/PublishingImages/FAM_750k_MapRelease_page.jpg.
- Kamerling, M.J., and Luyendyk, B.P., 1985, Paleomagnetism and Neogene tectonics of the northern Channel Islands, California: *Journal of Geophysical Research*, v. 90, p. 12,485–12,502, doi:10.1029/JB090iB14p12485.
- Kennedy, M.P., and Welday, E.E., 1980, Recency and character of faulting offshore metropolitan San Diego, California (San Diego Bay and immediate offshore shelf): *California Division of Mines and Geology Map Sheet 40*, scale 1:50,000.
- Kennedy, M.P., Clarke, S.H., Greene, H.G., and Legg, M.R., 1980, Recency and character of faulting offshore metropolitan San Diego, California (Point La Jolla to Mexico–U.S. international border): *California Division of Mines and Geology Map Sheet 42*, Scale 1:50,000.
- Kurt, H., et al., 2013, Steady late Quaternary slip rate on the Cinarcik section of the North Anatolian fault near Istanbul, Turkey: *Geophysical Research Letters*, v. 40, p. 4555–4559, doi:10.1002/grl.50882.
- Langenheim, V.E., Jachens, R.C., Graymer, R.W., Colgan, J.P., Wentworth, C.M., and Stanley, R.G., 2012, Fault geometry and cumulative offsets in the central Coast Ranges, California: Evidence for northward increasing slip along the San Gregorio–San Simeon–Hosgri fault: *Lithosphere*, v. 5, p. 29–48, doi:10.1130/L233.1.
- Legg, M.R., 1985, Geologic structure and tectonics of the inner continental borderland offshore northern Baja California, Mexico [Ph.D. thesis]: Santa Barbara, University of California, Santa Barbara, 410 p.
- Legg, M.R., 1991, Developments in understanding the tectonic evolution of the California Continental Borderland, in Osborne, R.H., ed., *From shoreline to abyss: Contributions in marine geology in honor of Francis Parker Shepard: SEPM (Society for Sedimentary Geology) Special Publication 46*, p. 291–312, doi:10.2110/pec.91.09.0291.
- Legg, M.R., Nicholson, C., Goldfinger, C., Milstein, R., and Kamerling, M.J., 2004, Large enigmatic crater structures offshore southern California: *Geophysical Journal International*, v. 159, p. 803–815, doi:10.1111/j.1365-246X.2004.02424.x.
- Lettis, W.R., and Hanson, K.L., 1991, Crustal strain partitioning: Implications for seismic-hazard assessment in western California: *Geology*, v. 19, p. 559–562, doi:10.1130/0091-7613(1991)019<0559:CSPIFS>2.3.CO;2.
- Lindvall, S.C., and Rockwell, T.K., 1995, Holocene activity of the Rose Canyon fault zone in San Diego, California: *Journal of Geophysical Research*, v. 100, p. 24,121–24,132, doi:10.1029/95JB02627.
- McDougall, K., Hillhouse, J., Powell, C., II, Mahan, S., Wan, E., and Sarna-Wojcicki, A.M., 2012, Paleontology and geochronology of the Long Beach core sites and monitoring wells, Long Beach, California: U.S. Geological Survey Open-File Report 2011-1274, 235 p.
- Mount, V.S., and Suppe, J., 1992, Present-day stress orientations adjacent to active strike-slip faults: California and Sumatra: *Journal of Geophysical Research*, v. 97, p. 11,995–12,013, doi:10.1029/92JB00130.
- Nicholson, C., 1996, Seismic behavior of the southern San Andreas fault zone in the northern Coachella Valley, California: Comparison of the 1948 and 1986 earthquake sequences: *Seismological Society of America Bulletin*, v. 86, p. 1331–1349.
- Nicholson, C., Sorlien, C.C., and Legg, M.R., 1993, Crustal imaging and extreme Miocene extension of the inner California Continental Borderland: *Geological Society of America Abstracts with Programs*, v. 25, no. 6, p. A-418.
- Nicholson, C., Sorlien, C.C., Atwater, T., Crowell, J.C., and Luyendyk, B.P., 1994, Microplate capture, rotation of the Western Transverse Ranges, and initiation of the San Andreas transform as a low-angle fault system: *Geology*, v. 22, p. 491–495, doi:10.1130/0091-7613(1994)022<0491:MCROTW>2.3.CO;2.
- Normark, W.R., Piper, D.J.W., Romans, B.W., Covault, J.A., Dartnell, P., and Sliter, R.W., 2009, Submarine canyon and fan systems of the California Continental Borderland, in Lee, H.J., and Normark, W.R., eds., *Earth science in the urban ocean: The Southern California Continental Borderland: Geological Society of America Special Paper 454*, p. 141–168, doi:10.1130/2009.2454(2.7).
- Plesch, A., et al., 2007, Community Fault Model (CFM) for southern California: *Seismological Society of America Bulletin*, v. 97, p. 1793–1802, doi:10.1785/0120050211.
- Ponti, D.J., et al., 2007, A 3-dimensional model of water-bearing sequences in the Dominguez Gap region, Long Beach, California: U.S. Geological Survey Open-File Report 2007-1013, 34 p.

- Rivero, C., and Shaw, J.H., 2011, Active folding and blind thrust faulting induced by basin inversion processes, inner California borderlands, *in* McClay, K., et al., eds., Thrust fault-related folding: American Association of Petroleum Geologists Memoir 94, p. 187–214, doi:10.1306/13251338M943432.
- Rivero, C., Shaw, J.H., and Mueller, K., 2000, Oceanside and Thirtymile Bank blind thrusts: Implications for earthquake hazards in coastal southern California: *Geology*, v. 28, p. 891–894, doi:10.1130/0091-7613(2000)28<891:OATBTT>2.0.CO;2.
- Roberts, A.P., 1995, Tectonic rotation about the termination of a major strike-slip fault, Marlborough fault system, New Zealand: *Geophysical Research Letters*, v. 22, p. 187–190, doi:10.1029/94GL02582.
- Ryan, H.F., Legg, M.R., Conrad, J.E., and Sliter, R.W., 2009, Recent faulting in the Gulf of Santa Catalina: San Diego to Dana Point, *in* Lee, H.J., and Normark, W.R., eds., Earth science in the urban ocean: The Southern California Continental Borderland: Geological Society of America Special Paper 454, p. 291–315, doi:10.1130/2009.2454(4.5).
- Ryan, H.F., Conrad, J.E., Paull, C.K., and McGann, M., 2012, Slip rate on the San Diego Trough fault zone, Inner California Borderland, and the 1986 Oceanside earthquake swarm revisited: *Seismological Society of America Bulletin*, v. 102, p. 2300–2312, doi:10.1785/0120110317.
- Schneider, C.L., Hummon, C., Yeats, R.S., and Huftile, G.L., 1996, Structural evolution of the northern Los Angeles basin, California, based on growth strata: *Tectonics*, v. 15, p. 341–355, doi:10.1029/95TC02523.
- Seeber, L., and Sorlien, C.C., 2000, Listric thrusts in the western Transverse Ranges, California: *Geological Society of America Bulletin*, v. 112, p. 1067–1079, doi:10.1130/0016-7606(2000)112<1067:LTITWT>2.0.CO;2.
- Seeber, L., Cormier, M.-H., McHugh, C., Emre, O., Polonia, A., and Sorlien, C., 2006, Subsidence and sedimentation at a transform bend: The Cinarcik Basin and the North Anatolian fault in the Marmara Sea, Turkey: *Geology*, v. 34, p. 933–936, doi:10.1130/G22520A.1.
- Şengör, A.M.C., Tüysüz, O., İmren, C., Sakıncı, M., Eyidoğan, H., Görür, N., Le Pichon, X., and Rangin, C., 2005, The North Anatolian fault: A new look: *Annual Review of Earth and Planetary Sciences*, v. 33, p. 37–112, doi:10.1146/annurev.earth.32.101802.120415.
- Sliter, R.W., Normark, W.R., and Gutmacher, C.E., 2005, Multichannel seismic-reflection data acquired off the coast of southern California—Part A 1997, 1998, 1999, and 2000: U.S. Geological Survey Open-File Report 2005-1084, <http://pubs.usgs.gov/of/2005/1084/>.
- Sliter, R.W., Ryan, H.F., and Triezenberg, P.J., 2010, High-resolution seismic reflection data offshore Dana Point, Southern California Borderland: U.S. Geological Survey Open-File Report 2010-1111, <http://pubs.usgs.gov/of/2010/1111/>.
- Sorlien, C.C., Nicholson, C., and Luyendyk, B.P., 1999, Miocene extension and post-Miocene transpression offshore of south-central California, *in* Keller, M.A., ed., Evolution of sedimentary basins/onshore oil and gas investigations—Santa Maria province: U. S. Geological Survey Bulletin 1995, 38 p.
- Sorlien, C.C., Kamerling, M.J., Seeber, L., and Broderick, K.G., 2006, Restraining segments and reactivation of the Santa Monica–Dume–Malibu Coast fault system, offshore Los Angeles, California: *Journal of Geophysical Research*, v. 111, B11402, doi:10.1029/2005JB003632.
- Sorlien, C.C., Campbell, B.A., and Seeber, L., 2010, Geometry, kinematics, and activity of a young mainland-dipping fold and thrust belt: Newport Beach to San Clemente, California: Final Report to U.S. Geological Survey NEHRP, contract USDI/USGS 08HQGR0103, 25 p., <http://earthquake.usgs.gov/research/external/reports/08HQGR0103.pdf>.
- Sorlien, C.C., Seeber, L., Broderick, K.G., Luyendyk, B.P., Fisher, M.A., Sliter, R.W., and Normark, W.R., 2013, The Palos Verdes Anticlinorium along the Los Angeles, California coast: Implications for underlying thrust faulting: *Geochemistry, Geophysics, Geosystems*, v. 14, p. 1866–1890, doi:10.1002/ggge.20112.
- Stuart, C.J., 1979, Lithofacies and origin of the San Onofre Breccia, coastal southern California, *in* Stuart, C. J., ed., A guidebook to Miocene lithofacies and depositional environments, coastal southern California and northwestern Baja California: Pacific Section, Society of Economic Paleontologists and Mineralogists, p. 25–42.
- Süss, M.P., and Shaw, J.H., 2003, P-wave seismic velocity structure derived from sonic logs and industry reflection data in the Los Angeles basin, California: *Journal of Geophysical Research*, v. 108, 2170, doi:10.1029/2001JB001628.
- Sylvester, A.G., 1988, Strike-slip faults: *Geological Society of America Bulletin*, v. 100, p. 1666–1703, doi:10.1130/0016-7606(1988)100<1666:SSF>2.3.CO;2.
- ten Brink, U.S., Zhang, J., Brocher, T.M., Okaya, D.A., Klitgord, K.D., and Fuis, G.S., 2000, Geophysical evidence for the evolution of the California Inner Continental Borderland as a metamorphic core complex: *Journal of Geophysical Research*, v. 105, p. 5835–5857, doi:10.1029/1999JB900318.
- Vedder, J.G., 1987, Regional geology and petroleum potential of the southern California borderland, *in* Scholl, D.W., et al., eds., Geology and resource potential of the continental margin of western North America and adjacent ocean basins, Beaufort Sea to Baja California: *Geology and resource potential of the continental margin of western North America and adjacent ocean basins, Beaufort Sea to Baja California*: Houston, Texas, Circum-Pacific Council for Energy and Mineral Resources, p. 403–447.
- Walker, R.G., 1975, Nested submarine-fan channels in the Capistrano Formation, California: *Geological Society of America Bulletin*, v. 86, p. 915–924, doi:10.1130/0016-7606(1975)86<915:NSCITC>2.0.CO;2.
- Willingham, C.R., Rietman, J.D., Heck, R.G., and Lettis, W.R., 2013, Characterization of the Hosgri fault zone and adjacent structures in the offshore Santa Maria Basin, south-central California, *in* Keller, M.A., ed., Evolution of sedimentary basins/onshore oil and gas investigations—Santa Maria province: U.S. Geological Survey Bulletin 1995, 105 p.
- Wright, T.L., 1991, Structural geology and tectonic evolution of the Los Angeles Basin, California, *in* Biddle, K.T., ed., Active margin basins: American Association of Petroleum Geologists Memoir 52, p. 35–134.
- Yeats, R.S., 1976, Extension versus strike-slip origin of the southern California Borderland, *in* Howell, D.G., ed., Aspects of the geological history of the California Borderland: American Association of Petroleum Geologists Publication 24, p. 455–485.
- Yeats, R.S., and Beall, J.M., 1991, Stratigraphic controls of oil fields in the Los Angeles basin, a guide to migration history, *in* Biddle, K.T., ed., Active margin basins: American Association of Petroleum Geologists Memoir 52, p. 221–235.